patients received RT or ASCT as first-line treatment. In addition, 3 of 7 patients who developed secondary malignancies received RT during the initial series of treatment. Among the secondary malignancies, myelodysplastic syndrome (MDS) or acute myeloblastic leukemia (AML) was reported in 2 patients. The patient who developed MDS received HDT/ASCT as a first-line treatment. The patient who developed AML received CHOP as a first-line treatment and ICE as a salvage treatment. Among the 187 patients treated with R-CHOP, 9 experienced cardiac toxicity, and 4 developed a secondary cancer. The median time to development of a secondary malignancy was 40.5 months (range 9-200 months).

Patients' characteristics and clinical outcomes in the R-CHOP group

Detailed characteristics of patients in the R-CHOP group are shown in *Online Supplementary Table S2*. We divided this group into four subgroups according to the disease status after R-CHOP or R-CHOP-like regimen and the presence or absence of consolidative RT: namely, R-CHOP+RT with residual mass, R-CHOP+RT in CR, R-CHOP with residual mass and R-CHOP in CR. Among the 187 patients in the R-CHOP group, 64 patients received consolidative RT after R-CHOP (*Online Supplementary Table S3*). Elderly age and higher IPI score were less common in those who received consolidative RT. Thirty-three of 64 patients received consolidative RT with residual mass after R-CHOP, while 31 of 64 patients received RT in CR after R-CHOP. Among the remaining 123 patients without consolidative RT, 34 patients did not achieve CR after R-CHOP, and 89 patients were in CR after R-CHOP, respectively. Among 34 patients with residual mass who were treated with R-CHOP, 16 patients developed progressive disease (PD), and 4 patients received follow up without RT based on the negative findings on PET/CT after the initial series of treatment. Of 89 patients who achieved a CR after R-CHOP but did not receive RT, 14 patients experienced relapse. Among these 14 patients, 9 developed the relapsed disease in their mediastinum, while the remaining 5 relapsed in other sites. The OS and PFS at four years of patients receiving consolidative RT were 100% and 85%, respectively, in the group with residual mass, and 96% and 90%, respectively, in the

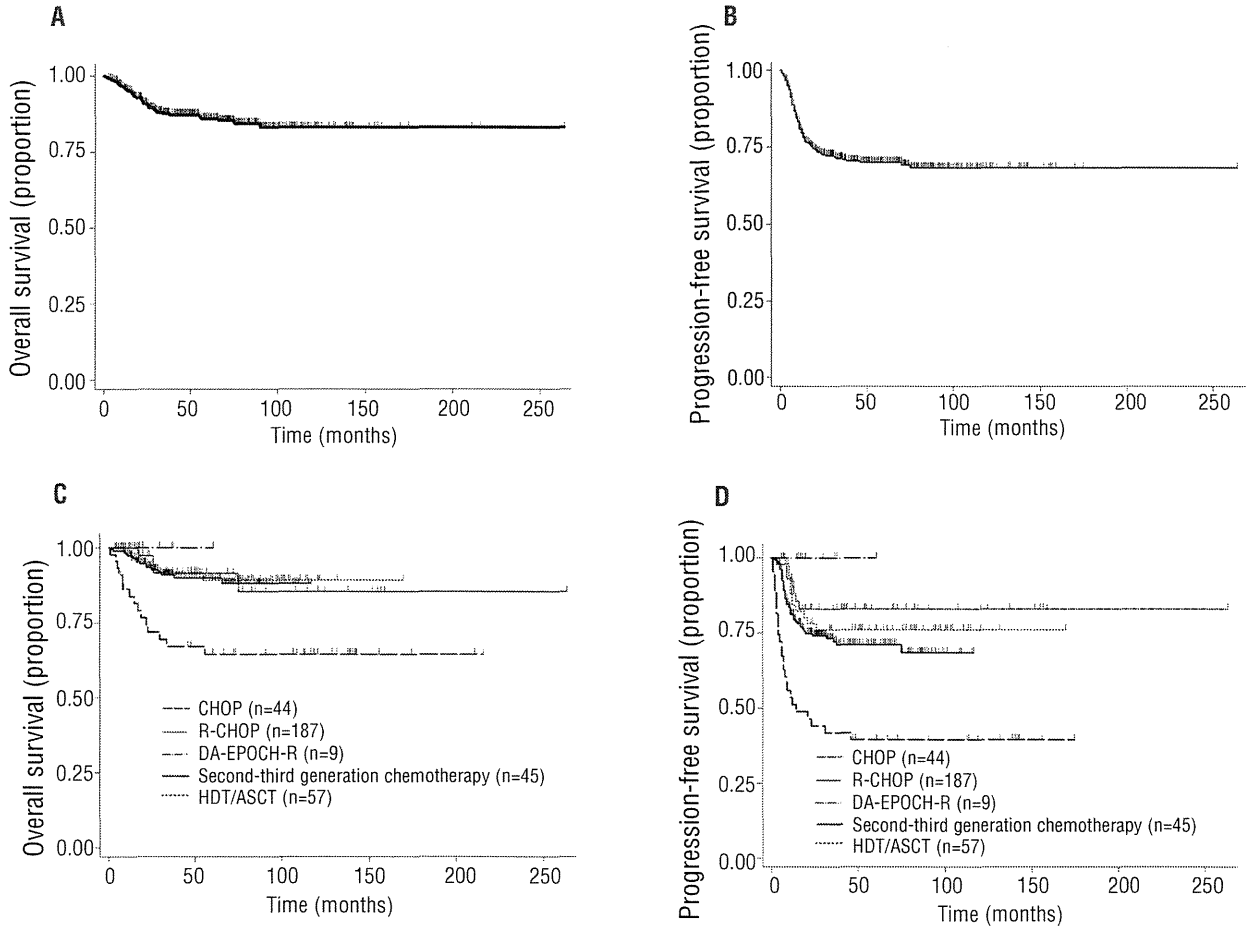

Figure 1. Survival of patients with primary mediastinal large B-cell lymphoma. (A) Overall survival (OS) of all patients with primary mediastinal large B-cell lymphoma (PMBL). (B) Progression-free survival (PFS) of all patients with PMBL. (C) OS of patients with PMBL treated with CHOP (n=44), R-CHOP (n=188), DA-EPOCH-R (n=9), 2nd- or 3rd-generation regimens (n=45), and HDT/ASCT (n=57). (D) PFS of patients with PMBL treated with CHOP (n=44), R-CHOP (n=188), DA-EPOCH-R (n=9), 2nd- or 3rd-generation regimens (n=45), and HDT/ASCT (n=57). CHOP: cyclophosphamide, adriamycin, vincristine and prednisone; R: rituximab; DA-EPOCH-R: dose-adjusted etoposide, cyclophosphosphamide, doxorubicin, vincristine, prednisolone and rituximab; HDT/ASCT: high-dose chemotherapy followed by autologous stem cell transplantation.

group in CR (OS: P=0.15; PFS: P=0.80) (*Online Supplementary Figures S1 and S2*). Meanwhile, the OS and PFS at four years of patients who did not receive consolidative RT were 64% and 35%, respectively, in the group with residual mass without disease progression, and 95% and 77%, respectively, in the group in CR (OS: P<0.001; PFS: P<0.001). Taken together, these data indicate that a significant proportion of patients achieving CR after R-CHOP can be cured without consolidative RT.

Prognostic factors and survival for patients treated with R-CHOP and without consolidative radiotherapy

One hundred and twenty-three patients receiving R-CHOP without consolidative RT were analyzed. The analysis of potential prognostic factors is shown in Table 2. On univariate analysis, the presence of pleural or pericardial effusion, performance status (PS) over 1 and higher IPI were adverse prognostic factors for OS, and the presence of pleural or pericardial effusion, advanced stage, extranodal involvement, PS, LDH, soluble interleukin-2 receptor (sIL-2R), and higher IPI were adverse prognostic factors for PFS. On multivariate analysis, we could not identify significant prognostic factors for OS. The presence of pleural or pericardial effusion [hazard ratio (HR), 3.53; 95% confidence interval (CI), 1.69-7.40; P=0.001] and advanced stage (stage III/IV; HR, 2.16; 95%CI: 1.14-4.11; P=0.018) were identified as adverse prognostic factors for PFS. As almost all the patients with progression after R-CHOP developed disease within 12 months after diagnosis, we performed Cox regression analyses to determine the predictive factors for primary refractory or early relapse within 12 months after diagnosis. On multivariate analysis, only the presence of pleural or pericardial effusion was predictive of primary refractory or early relapse within 12 months (HR, 6.11; 95%CI: 2.30-16.24; P<0.001). In this cohort, only 5 (8%) of 65 patients without pleural or pericardial effusion experienced primary refractory or early relapse within 12 months; meanwhile, 25 (43%) of 58 patients with pleural or pericardial effusion (P<0.001) had refractory or early relapsed disease.

As IPI and the presence of pleural or pericardial effusion were prognostic factors for OS on univariate analysis, and these were not related (correlation coefficient = 0.39), the OS and PFS in patients receiving R-CHOP without RT were analyzed according to these prognostic factors. The OS and PFS in patients receiving R-CHOP without RT were analyzed according to the presence of pleural or pericardial effusion and IPI. As expected (Figure 2A and B), the best OS and PFS were observed in patients with low IPI and without pleural or pericardial effusion. The OS and

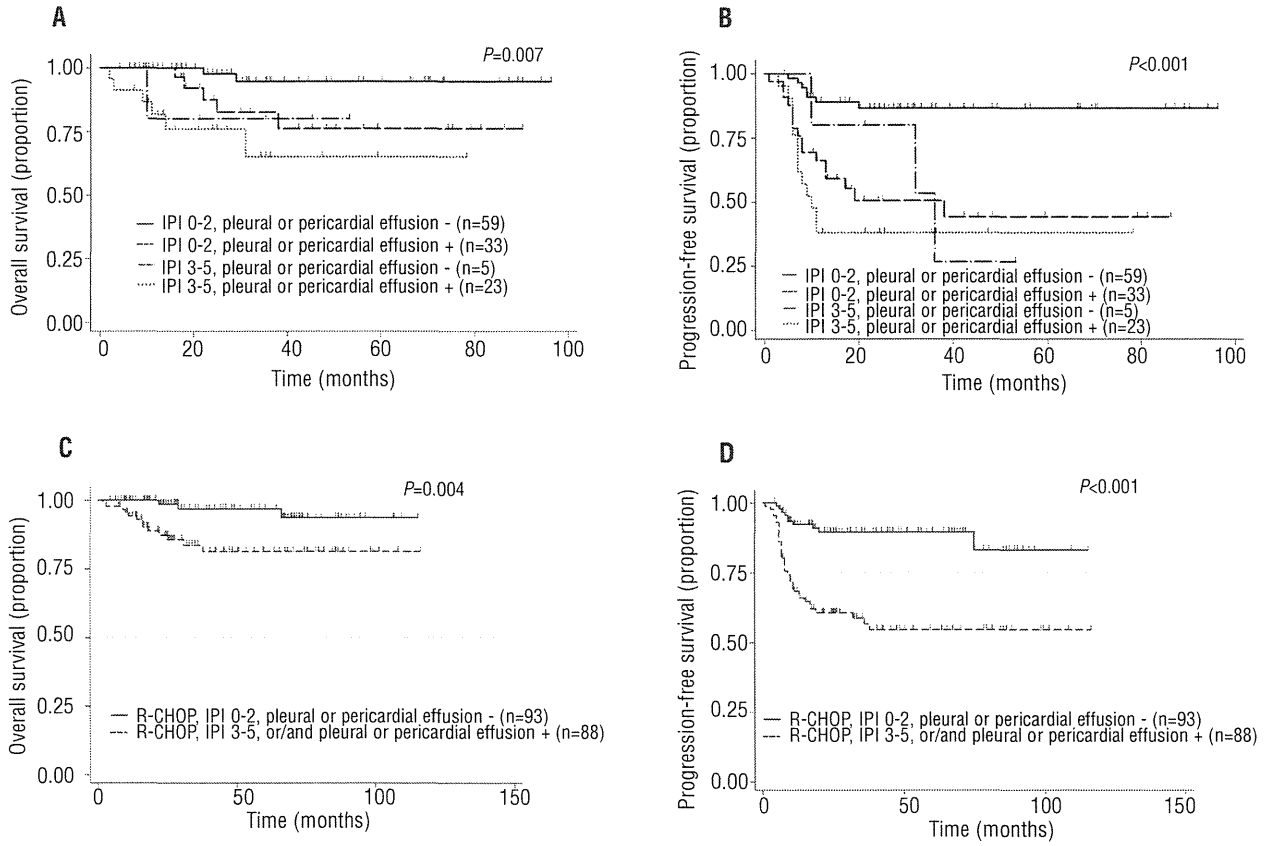

Figure 2. Survival of patients with primary mediastinal large B-cell lymphoma according to the International Prognostic Index and the presence pleural or pericardial effusion. (A) Overall survival (OS) of patients with primary mediastinal large B-cell lymphoma (PMBL) treated with R-CHOP without radiation therapy (RT) according to the international prognostic index (IPI) and the presence pleural or pericardial effusion. (B) Progression-free survival (PFS) of patients with PMBL treated with R-CHOP without RT according to the IPI and the presence pleural or pericardial effusion. (C) OS of patients with PMBL treated with R-CHOP according to the IPI and the presence pleural or pericardial effusion. (D) PFS of patients with PMBL treated with R-CHOP according to the IPI and the presence pleural or pericardial effusion. R-CHOP: rituximab, cyclophosphamide, adriamycin, vincristine and prednisone; RT: radiation therapy.

PFS at four years of these 58 patients were 95% and 87%, respectively. Meanwhile, based on individual factors of LDH, B symptom, and pleural or pericardial effusion identified on multivariate analysis for PFS, the OS and PFS were also analyzed (*Online Supplementary Figures S3 and S4*). Although the OS and PFS could be well stratified, the number of patients categorized into the well stratified low-risk category was lower than that of patients under the stratification using IPI and effusion. Taken together, these data indicate that a significant proportion of patients with low IPI and without pleural or pericardial effusion at the time of diagnosis can be potentially cured by the R-CHOP regimen without consolidative RT.

Meanwhile, the treatment should be considered for patients with higher IPI and the presence of pleural or pericardial effusion. As shown in Figure 2C and D, the outcomes of R-CHOP were not satisfactory in patients with higher IPI and/or the presence of pleural or pericardial effusion (4-year OS: 97% *vs.* 81%, P=0.004; 4-year PFS: 89% *vs.* 54%, P<0.001, respectively).

Discussion

It is important to establish a more effective and less toxic standard treatment for PMBL, as affected patients tended to be young and can be cured when properly treated. The present study investigated a larger cohort than other studies and indicated that almost all PMBL patients with lower IPI and the absence of the pleural or pericardial effusion could be cured by the R-CHOP regimen without consolidative RT. Considering the excellent outcomes of the recent promising regimen DA-EPOCH-R, reported by Dunleavy *et al.*,[27] the initial treatment regimen for PMBL could be stratified according to our simple indicators of IPI score and the presence of pleural or pericardial effusion; DA-EPOCH-R or R-CHOP could be selected for high- or low-risk PMBL patients, respectively.

Consistent with other studies, patients who received rituximab-containing chemotherapies showed better outcomes.[17-22,27,35] HDT/ASCT and 2nd-/3rd-generation regimens that were more intensive and that have been historically used as first-line treatment for PMBL resulted in better outcomes than those seen in response to CHOP chemotherapy.[11,17,18,36] In the present study, similar OS and PFS was observed among patients treated with a 2nd-/3rd-generation regimen, HDT/ASCT, and R-CHOP. This suggests that R-CHOP regimen might have curative potential in a significant proportion of PMBL patients without utilizing 2nd-/3rd-generation regimen or HDT/ASCT and thereby avoiding their associated toxicities.

Late toxicities are another important issue to consider when weighing the benefits of different curative regimens. In the current study, 17 patients had late adverse events (secondary cancer, n=7; cardiac toxicity, n=10). Previous reports indicated that RT to the mediastinum significantly increased the risk of breast cancer and cardiac toxicity.[24-26,37] Although longer follow up is required to evaluate for late toxicities, we investigated whether we could omit the consolidative RT from the current treatment strategies. We analyzed the outcomes of patients treated with R-CHOP without consolidative RT, and identified higher IPI and the presence of pleural or pericardial effusion as adverse risk factors for OS. Moreover, the presence of the effusion was identified as an adverse risk factor for early relapse. Considering that previous studies had reported that the presence of pleural effusion was associated with poor outcomes in patients with PMBL and Hodgkin lymphoma,[21,38] our results might be universal. Our simple indicators could identify patients who could be cured in response to R-CHOP without consolidative RT; however, patients with these factors comprised only approximately one-half of patients receiving R-CHOP. This means the remaining patients should be treated with an alternative regimen. The fact that excellent outcomes were seen in patients with higher IPI and the presence of the effusion receiving DA-EPOCH-R regimen in this study, as well as in another recent report,[27] suggests that it may be reasonable to use this approach in high-risk PMBL patients. A prospective trial of this strategy is warranted.

Another approach to stratify PMBL patients is currently being investigated in Europe. The prospective IELSG-37 trial is investigating whether consolidative RT could be omitted according to the presence or absence of FDG-PET or PET/CT findings after the initial series of treatments. In clinical practice, we frequently encounter patients in whom it is difficult to judge FDG-PET positivity.[39,40] Unfortunately, we could not evaluate the role of PET/CT in this study because of retrospective settings. Meanwhile, the very recent report from the IELSG-26 study clarified the role of PET/CT after treatment in PMBL patients.[41] Considering the difficulty of re-biopsy of the suspected mediastinal mass after treatment, using the optimal cut-off value on PET/CT after treatment reported by IELSG could be an important tool to assess the risk of treatment failure.

This study has several limitations. First, its retrospective nature might have unrecognized biases and the results should be interpreted with care. Regarding evaluation of response, evaluation of the residual mass might have been heterogeneous at each institution because of the retrospective setting. Therefore, the CR rate in our study could be over-estimated. Second, patients received various treatment regimens and consolidative RT according to each institution's preferred strategy; thus, treatment outcomes might have been over-estimated or under-estimated. In particular, patients who did not receive consolidative RT might have had clinical indicators that physicians considered favorable, resulting in an overestimation of the clinical outcomes in response to R-CHOP without consolidative RT. However, in the present analysis, the proportion of patients with higher IPI and with the presence of effusion was not low in patients who did not receive consolidative RT compared with that in patients who did receive RT. This suggests that the base-line characteristics and outcomes of patients without consolidative RT were not necessarily favorable and that they might not have been over-estimated. Finally, we carried out a central pathological review for only 196 patients. We tried to collect as much pathological histological paraffin-embedded tissue materials as possible. However, in some cases, sufficient materials were not available because they were too old. In addition, the period during which data could be submitted differed because clinical data were kept for different lengths of time at the different institutions. Therefore, the number of institutions who could submit clinical data in the 1980s and 1990s was smaller than in the 2000s: 10 and 65 institutions before and after the year 2000, respectively. Furthermore, although gene expression or methylation profiling can help to diagnose PMBL correctly, for the moment we cannot use these tools in routine clinical prac-

tice. Further study of the utility of these biological tools is necessary to improve diagnosis and management of this disease.

In conclusion, the present study demonstrated that IPI and the presence of pleural or pericardial effusion were adverse prognostic factors for risk stratification of PMBL patients treated with R-CHOP. R-CHOP without consolidative RT can achieve a high rate of cure for approximately one-half of PMBL patients, while alternative regimens, including DA-EPOCH-R, should be offered to the remaining patients. Prospective studies to validate these prognostic factors and a risk-adopted treatment strategy are warranted.

Acknowledgments

The authors would like to thank following physicians for providing patient cases; Yoshinobu Kanda, MD of Saitama Medical Center, Jichi Medical University, Yoshihiro Yakushizin, MD of Ehime University Hospital, Yasunori Nakagawa, MD of the Japanese Red Cross Medical Center, Taro Masunari, MD of Chugoku Central Hospital, Yoshitoyo Kagami, MD of Toyota Kosei Hospital, Kazunori Ohnishi, MD of Hamamatsu University Hospital, Naoe Goto, MD of Gifu University Hospital, Norifumi Tsukamoto, MD of Gunma University Hospital, Noriyasu Fukushima, MD of Saga University Hospital, Shigeru Kusumoto, MD of Nagoya City University Hospital, Yoshitaka Imaizumi, MD of Nagasaki University Hospital, Koji Kato, MD of Kyushu University Hospital, Takenori Takahata, MD of Hirosaki University Hospital, Yasufumi Masaki, MD of Kanazawa Medical University Hospital, Akiyo Yoshida, MD of Kanazawa University Hospital, Masanobu Nakata, MD of Sapporo Hokuyu Hospital, Akinao Okamoto, MD of Fujita Health University Hospital, Ryosuke Shirasaki, MD of Teikyo University Hospital, Ichiro Hanamura, MD of Aichi Medical University Hospital, Kensuke Naito, MD of Hamamatsu Medical Center, Shingo Kurahashi, MD of Japanese Red Cross Nagoya First Hospital, Masahide Yamamoto, MD of Medical Hospital of Tokyo Medical and Dental University, Junji Suzumiya, MD of Shimane University Hospital, Hirokazu Nagai, MD of Nagoya Medical Center, Masahiro Yokoyama, MD of Cancer Institute Hospital, Yuichi Hasegawa, MD of University of Tsukuba Hospital, Katsuhiro Miura, MD of Nihon University Itabashi Hospital, Kensuke Usuki, MD of NTT Medical Center Tokyo, Naokuni Uike, MD of Kyushu Cancer Center, Shin Fujisawa, MD of Yokohama City University Medical Center, Yasushi Takamatsu, MD of Fukuoka University Hospital, Akinori Nishikawa, MD of Wakayama Medical University Hospital, Naoto Tomita, MD of Yokohama City University Hospital, Hideki Tsujimura, MD of Chiba Cancer Center, Takashi Miyagi, MD of Heart Life Hospital, Katsuya Fujimoto, MD of Hokkaido University Hospital, Senji Kasahara, MD of Gifu Municipal Hospital, Atsushi Wakita, MD of Nagoya City West Medical Center, Michihide Tokuhira, MD of Saitama Medical Center, Takahiko Utsumi, MD of Shiga Medical Center for Adults, Kazuhito Yamamoto, MD of Aichi Cancer Center, Kunio Kitamura, MD of Ichinomiya Municipal Hospital, Toshimasa Kamoda, MD of Tenri Hospital, Kana Miyazaki, MD of Mie University Hospital, Keiichiro Mihara, MD of Hiroshima University Hospital, Yoshiko Inoue, MD of Kumamoto Medical Center, Masatoshi Kanno, MD of Nara Medical University Hospital, Kazutaka Sunami, MD of Okayama Medical Center, Noriko Usui, MD of Third Hospital, Jikei University School of Medicine, and Yoshiharu Maeda, MD of Komagome Hospital.; and We thank Tomomitsu Hotta, MD, of the National Cancer Center for critical reading of the manuscript. We also thank the patients, physicians, nurses, and staff members who participated in this multicenter trial for their excellent cooperation.

Funding

This work was supported by the Hematological Malignancy Clinical Study Group and the National Cancer Center Research and Development Fund (23-A-17).

Authorship and Disclosures

Information on authorship, contributions, and financial & other disclosures was provided by the authors and is available with the online version of this article at www.haematologica.org.

References

1. Swerdlow S, Campo E, Harris N, Jaffe E, Pileri S, Stein H, et al. WHO Classification of Tumours of Haematopoietic and Lymphoid Tissues. Lyon, France: IARC Press;. 2008.
2. Cazals-Hatem D, Lepage E, Brice P, Ferrant A, d'Agay MF, Baumelou E, et al. Primary mediastinal large B-cell lymphoma. A clinicopathologic study of 141 cases compared with 916 nonmediastinal large B-cell lymphomas, a GELA ("Groupe d'Etude des Lymphomes de l'Adulte") study. Am J Surg Pathol. 1996;20(7):877-88.
3. Lazzarino M, Orlandi E, Paulli M, Strater J, Klersy C, Gianelli U, et al. Treatment outcome and prognostic factors for primary mediastinal (thymic) B-cell lymphoma: a multicenter study of 106 patients. J Clin Oncol. 1997;15(4):1646-53.
4. van Besien K, Kelta M, Bahaguna P. Primary mediastinal B-cell lymphoma: a review of pathology and management. J Clin Oncol. 2001;19(6):1855-64.
5. Zinzani PL, Martelli M, Bertini M, Gianni AM, Devizzi L, Federico M, et al. Induction chemotherapy strategies for primary mediastinal large B-cell lymphoma with sclerosis: a retrospective multinational study on 426 previously untreated patients. Haematologica. 2002;87(12):1258-64.
6. Hamlin PA, Portlock CS, Straus DJ, Noy A, Singer A, Horwitz SM, et al. Primary mediastinal large B-cell lymphoma: optimal therapy and prognostic factor analysis in 141 consecutive patients treated at Memorial Sloan Kettering from 1980 to 1999. Br J Haematol. 2005;130(5):691-9.
7. Martelli MP, Martelli M, Pescarmona E, De Sanctis V, Donato V, Palombi F, et al. MACOP-B and involved field radiation therapy is an effective therapy for primary mediastinal large B-cell lymphoma with sclerosis. Ann Oncol. 1998;9(9):1027-9.
8. Todeschini G, Ambrosetti A, Meneghini V, Pizzolo G, Menestrina F, Chilosi M, et al. Mediastinal large-B-cell lymphoma with sclerosis: a clinical study of 21 patients. J Clin Oncol. 1990;8(5):804-8.
9. Zinzani PL, Martelli M, Bendandi M, De Renzo A, Zaccaria A, Pavone E, et al. Primary mediastinal large B-cell lymphoma with sclerosis: a clinical study of 89 patients treated with MACOP-B chemotherapy and radiation therapy. Haematologica. 2001;86(2):187-91.
10. Zinzani PL, Martelli M, Magagnoli M, Pescarmona E, Scaramucci L, Palombi F, et al. Treatment and clinical management of primary mediastinal large B-cell lymphoma with sclerosis: MACOP-B regimen and mediastinal radiotherapy monitored by (67)Gallium scan in 50 patients. Blood. 1999;94(10):3289-93.
11. Sehn LH, Antin JH, Shulman LN, Mauch P, Elias A, Kadin ME, et al. Primary diffuse large B-cell lymphoma of the mediastinum: outcome following high-dose chemotherapy and autologous hematopoietic cell transplantation. Blood. 1998;91(2):717-23.
12. Cairoli R, Grillo G, Tedeschi A, Gargantini L, Marenco P, Tresoldi E, et al. Efficacy of an early intensification treatment integrating chemotherapy, autologous stem cell transplantation and radiotherapy for poor risk primary mediastinal large B cell lymphoma with sclerosis. Bone Marrow Transplant. 2002;29(6):473-7.
13. Witzens-Harig M, Ho AD, Kuhnt E, Trneny M, Rieger M, Osterborg A, et al. Primary

Mediastinal B Cell Lymphoma Treated with CHOP-Like Chemotherapy with or without Rituximab: 5-Year Results of the Mabthera International Trial Group (MInT) Study. ASH Annual Meeting Abstracts. 2012;120(21):1612.
14. Shimada K, Matsue K, Yamamoto K, Murase T, Ichikawa N, Okamoto M, et al. Retrospective analysis of intravascular large B-cell lymphoma treated with rituximab-containing chemotherapy as reported by the IVL study group in Japan. J Clin Oncol. 2008;26(19):3189-95.
15. Pfreundschuh M, Schubert J, Ziepert M, Schmits R, Mohren M, Lengfelder E, et al. Six versus eight cycles of bi-weekly CHOP-14 with or without rituximab in elderly patients with aggressive CD20+ B-cell lymphomas: a randomised controlled trial (RICOVER-60). Lancet Oncol. 2008; 9(2):105-16.
16. Coiffier B, Lepage E, Briere J, Herbrecht R, Tilly H, Bouabdallah R, et al. CHOP chemotherapy plus rituximab compared with CHOP alone in elderly patients with diffuse large-B-cell lymphoma. N Engl J Med. 2002;346(4):235-42.
17. Savage KJ, Al-Rajhi N, Voss N, Paltiel C, Klasa R, Gascoyne RD, et al. Favorable outcome of primary mediastinal large B-cell lymphoma in a single institution: the British Columbia experience. Ann Oncol. 2006;17(1):123-30.
18. Zinzani PL, Stefoni V, Finolezzi E, Brusamolino E, Cabras MG, Chiappella A, et al. Rituximab combined with MACOP-B or VACOP-B and radiation therapy in primary mediastinal large B-cell lymphoma: a retrospective study. Clin Lymphoma Myeloma. 2009;9(5):381-5.
19. Rieger M, Osterborg A, Pettengell R, White D, Gill D, Walewski J, et al. Primary mediastinal B-cell lymphoma treated with CHOP-like chemotherapy with or without rituximab: results of the Mabthera International Trial Group study. Ann Oncol. 2011;22(3):664-70.
20. Tai WM, Quah D, Yap SP, Tan SH, Tang T, Tay KW, et al. Primary mediastinal large B-cell lymphoma: optimal therapy and prognostic factors in 41 consecutive Asian patients. Leuk Lymphoma. 2011;52(4): 604-12.
21. Savage KJ, Yenson PR, Shenkier T, Klasa R, Villa D, Goktepe O, et al. The Outcome of Primary Mediastinal Large B-Cell Lymphoma (PMBCL) in the R-CHOP Treatment Era. ASH Annual Meeting Abstracts. 2012;120(21):303.
22. Vassilakopoulos TP, Pangalis GA, Katsigiannis A, Papageorgiou SG, Constantinou N, Terpos E, et al. Rituximab, cyclophosphamide, doxorubicin, vincristine, and prednisone with or without radiotherapy in primary mediastinal large B-cell lymphoma: the emerging standard of care. Oncologist. 2012;17(2):239-49.
23. Xu LM, Fang H, Wang WH, Jin J, Wang SL, Liu YP, et al. Prognostic significance of rituximab and radiotherapy for patients with primary mediastinal large B-cell lymphoma receiving doxorubicin-containing chemotherapy. Leuk Lymphoma. 2013; 54(8):1684-90.
24. Galper SL, Yu JB, Mauch PM, Strasser JF, Silver B, Lacasce A, et al. Clinically significant cardiac disease in patients with Hodgkin lymphoma treated with mediastinal irradiation. Blood. 2011;117(2):412-8.
25. Henderson TO, Amsterdam A, Bhatia S, Hudson MM, Meadows AT, Neglia JP, et al. Systematic review: surveillance for breast cancer in women treated with chest radiation for childhood, adolescent, or young adult cancer. Ann Intern Med. 2010; 152(7):444-55; W144-54.
26. Nieder C, Schill S, Kneschaurek P, Molls M. Comparison of three different mediastinal radiotherapy techniques in female patients: Impact on heart sparing and dose to the breasts. Radiother Oncol. 2007;82(3):301-7.
27. Dunleavy K, Pittaluga S, Maeda LS, Advani R, Chen CC, Hessler J, et al. Dose-adjusted EPOCH-rituximab therapy in primary mediastinal B-cell lymphoma. N Engl J Med. 2013;368(15):1408-16.
28. Yamamoto W, Nakamura N, Tomita N, Ishii Y, Takasaki H, Hashimoto C, et al. Clinicopathological analysis of mediastinal large B-cell lymphoma and classical Hodgkin lymphoma of the mediastinum. Leuk Lymphoma. 2013;54(5):967-72.
29. Yamamoto W, Nakamura N, Tomita N, Ishii Y, Takasaki H, Hashimoto C, et al. Clinicopathological analysis of mediastinal large B-cell lymphoma and classical Hodgkin lymphoma of the mediastinum. Leuk Lymphoma. 2013;54(5):967-72.
30. Hu S, Xu-Monette ZY, Balasubramanyam A, Manyam GC, Visco C, Tzankov A, et al. CD30 expression defines a novel subgroup of diffuse large B-cell lymphoma with favorable prognosis and distinct gene expression signature: a report from the International DLBCL Rituximab-CHOP Consortium Program Study. Blood. 2013; 121(14):2715-24.
31. Hans CP, Weisenburger DD, Greiner TC, Gascoyne RD, Delabie J, Ott G, et al. Confirmation of the molecular classification of diffuse large B-cell lymphoma by immunohistochemistry using a tissue microarray. Blood. 2004;103(1):275-82.
32. Cheson BD, Horning SJ, Coiffier B, Shipp MA, Fisher RI, Connors JM, et al. Report of an international workshop to standardize response criteria for non-Hodgkin's lymphomas. NCI Sponsored International Working Group. J Clin Oncol. 1999; 17(4):1244.
33. Niitsu N, Okamoto M, Aoki S, Okumura H, Yoshino T, Miura I, et al. Multicenter phase II study of the CyclOBEAP (CHOP-like + etoposide and bleomycin) regimen for patients with poor-prognosis aggressive lymphoma. Ann Hematol. 2006;85(6):374-80.
34. Yamada Y, Tomonaga M, Fukuda H, Hanada S, Utsunomiya A, Tara M, et al. A new G-CSF-supported combination chemotherapy, LSG15, for adult T-cell leukaemia-lymphoma: Japan Clinical Oncology Group Study 9303. Br J Haematol. 2001;113(2):375-82.
35. Barth TF, Leithauser F, Joos S, Bentz M, Moller P. Mediastinal (thymic) large B-cell lymphoma: where do we stand? Lancet Oncol. 2002;3(4):229-34.
36. Rodriguez J, Conde E, Gutierrez A, Garcia-Ruiz JC, Lahuerta JJ, Varela MR, et al. Front-Line Autologous Stem Cell Transplantation (ASCT) in Primary Mediastinal Large B-Cell Lymphoma: The GEL-TAMO Experience. ASH Annual Meeting Abstracts. 2006;108(11):3056-.
37. Meyer RM, Gospodarowicz MK, Connors JM, Pearcey RG, Wells WA, Winter JN, et al. ABVD alone versus radiation-based therapy in limited-stage Hodgkin's lymphoma. N Engl J Med. 2012;366(5):399-408.
38. Hunter BD, Dhakal S, Voci S, Goldstein NP, Constine LS. Pleural effusions in patients with Hodgkin lymphoma: clinical predictors and associations with outcome. .Leuk Lymphoma. 2014;55(8):1822-6.
39. Filippi AR, Piva C, Giunta F, Bello M, Chiappella A, Caracciolo D, et al. Radiation therapy in primary mediastinal B-cell lymphoma with positron emission tomography positivity after rituximab chemotherapy. Int J Radiat Oncol Biol Phys. 2013; 87(2):311-6.
40. Woessmann W, Lisfeld J, Burkhardt B. Therapy in primary mediastinal B-cell lymphoma. N Engl J Med. 2013;369(3):282.
41. Martelli M, Ceriani L, Zucca E, Zinzani PL, Ferreri AJ, Vitolo U, et al. [18F]fluorodeoxyglucose positron emission tomography predicts survival after chemoimmunotherapy for primary mediastinal large B-cell lymphoma: results of the International Extranodal Lymphoma Study Group IELSG-26 Study. J Clin Oncol. 2014; 32(17):1769-75.

Target Antigen Density Governs the Efficacy of Anti–CD20-CD28-CD3 ζ Chimeric Antigen Receptor–Modified Effector CD8$^+$ T Cells

Keisuke Watanabe,*,[1] Seitaro Terakura,*,[1] Anton C. Martens,[†,‡] Tom van Meerten,[§] Susumu Uchiyama,[¶] Misa Imai,[‖] Reona Sakemura,* Tatsunori Goto,* Ryo Hanajiri,* Nobuhiko Imahashi,* Kazuyuki Shimada,*,[#] Akihiro Tomita,* Hitoshi Kiyoi,* Tetsuya Nishida,* Tomoki Naoe,*,** and Makoto Murata*

The effectiveness of chimeric Ag receptor (CAR)–transduced T (CAR-T) cells has been attributed to supraphysiological signaling through CARs. Second- and later-generation CARs simultaneously transmit costimulatory signals with CD3ζ signals upon ligation, but may lead to severe adverse effects owing to the recognition of minimal Ag expression outside the target tumor. Currently, the threshold target Ag density for CAR-T cell lysis and further activation, including cytokine production, has not yet been investigated in detail. Therefore, we determined the threshold target Ag density required to induce CAR-T cell responses using novel anti-CD20 CAR-T cells with a CD28 intracellular domain and a CD20-transduced CEM cell model. The newly developed CD20CAR–T cells demonstrated Ag-specific lysis and cytokine secretion, which was a reasonable level as a second-generation CAR. For lytic activity, the threshold Ag density was determined to be ~200 molecules per target cell, whereas the Ag density required for cytokine production of CAR-T cells was ~10-fold higher, at a few thousand per target cell. CD20CAR–T cells responded efficiently to CD20-downregulated lymphoma and leukemia targets, including rituximab- or ofatumumab-refractory primary chronic lymphocytic leukemia cells. Despite the potential influence of the structure, localization, and binding affinity of the CAR/Ag, the threshold determined may be used for target Ag selection. An Ag density below the threshold may not result in adverse effects, whereas that above the threshold may be sufficient for practical effectiveness. CD20CAR–T cells also demonstrated significant lytic activity against CD20-downregulated tumor cells and may exhibit effectiveness for CD20-positive lymphoid malignancies. *The Journal of Immunology*, **2015, 194: 911–920.**

Chimeric Ag receptor (CAR)–transduced T (CAR-T) cell therapy is an emerging therapeutic strategy for refractory acute lymphoblastic leukemia (ALL) and chronic lymphocytic leukemia (CLL) (1, 2). Second- and later-generation CARs generally consist of a single-chain variable fragment (scFv) from a mAb fused to the signaling domain of CD3ζ, and contain one or two costimulatory endodomains, respectively (3–5). This technology has two main potential benefits over TCR gene insertion. One is that Ag recognition by CAR is independent of HLA, meaning that CAR therapy can be used to treat all Ag-positive patients regardless of their HLA. The other is that once CARs ligate to target molecules, full activation signals, including costimuli such as CD28 or 4-1BB, are transmitted to CAR-T cells (3–5). A superior effector function and proliferation following activation have been reported in second- and third-generation CAR-T cells (6–9).

In contrast, CAR-T cells may induce adverse effects by recognizing low expression levels of the target Ag in an off-target organ. This activity has been referred to as the "on-target/off-tumor effect." A serious adverse event induced by CAR-T cells, which recognize very low expression levels of ERBB2 on lung epithelial cells, was reported with CAR therapy targeting ERBB2 based on trastuzumab (Herceptin) (10). Although ERBB2 is expressed at low levels in various normal tissues, including lung, the anti-ERBB2 humanized mAb trastuzumab has been used safely in clinical settings (11), indicating that ERBB2 expression levels on lung cells are negligible in terms of trastuzumab therapy (12). However, ERBB2–CAR-T cells induce significant Ag-specific responses against this low expression of ERBB2 (10, 11). Therefore, selection of a target Ag is critical for both efficacy and avoiding adverse effects. TCRs recognize very low numbers of peptide/HLA complexes, whereas a relatively high number of target molecules are required for mAbs to induce cytotoxic activity (13, 14). However, the range of Ag density in which CAR-T

*Department of Hematology and Oncology, Nagoya University Graduate School of Medicine, Nagoya 466-8560, Japan; [†]Department of Hematology, VU University Medical Center Amsterdam, 1007 MB Amsterdam, the Netherlands; [‡]Department of Immunology, University Medical Center Utrecht, 3508 GA Utrecht, the Netherlands; [§]Department of Hematology, University Medical Center Groningen, 9700 RB Groningen, the Netherlands; [¶]Division of Advanced Science and Biotechnology, Graduate School of Engineering, Osaka University, Osaka 565-0871, Japan; [‖]Faculty of Pharmacy, Meijo University, Nagoya 468-8503, Japan; [#]Institute for Advanced Research, Nagoya University, Nagoya 464-8601, Japan; and **National Hospital Organization Nagoya Medical Center, Nagoya 460-0001, Japan

[1]K.W. and S.T. contributed equally to this work.

Received for publication September 12, 2014. Accepted for publication November 21, 2014.

This work was supported by grants from the Foundation for Promotion of Cancer Research (Tokyo, Japan; to S.T.), the Japan Society for the Promotion of Science KAKENHI (24790969 to S.T.), the Program to Disseminate Tenure Tracking System (MEXT, Japan; to K.S.), a Grant-in-Aid for Challenging Exploratory Research (23659487 to T. Naoe), and a Health Labor Science Research Grant (H25-Immunology-104 to M.M.).

The online version of this article contains supplemental material.

Address correspondence and reprint requests to Dr. Seitaro Terakura, Department of Hematology and Oncology, Nagoya University Graduate School of Medicine, 65 Tsurumai, Showa-ku, Nagoya, Aichi 466-8560, Japan. E-mail address: tseit@med.nagoya-u.ac.jp

Abbreviations used in this article: ABC, Ab-binding capacity; ADCC, Ab-dependent cellular cytotoxicity; ALL, acute lymphoblastic leukemia; CAR, chimeric Ag receptor; CAR-T, CAR-transduced T (cell); CDC, complement-dependent cytotoxicity; CLL, chronic lymphocytic leukemia; DLBCL, diffuse large B cell lymphoma; FCM, flow cytometry; LCL, EBV-transformed lymphoblastoid cell line; MFI, mean fluorescence intensity; ofa, ofatumumab; sABC, specific Ab binding capacity; scFv, single-chain variable fragment; tEGFR, truncated version of the epidermal growth factor receptor.

www.jimmunol.org/cgi/doi/10.4049/jimmunol.1402346

cells can recognize and induce cytotoxicity has not been investigated in detail. Furthermore, research has not yet clarified the number of Ag molecules expressed that could be candidates for targets when expressed at low levels or that should be avoided owing to the on-target/off-tumor effect (15).

CD20 is an activated glycosylated phosphoprotein that is expressed on the surface of B lymphocytes. An anti-CD20 mAb is an effective therapeutic option for various B cell malignancies such as ALL (16), CLL (17), and malignant lymphoma (18, 19). Although combination chemotherapies with rituximab have achieved favorable results in CD20-positive B cell lymphoma patients, acquired resistance to rituximab has become a problem, with a suggested mechanism of reduced expression of CD20 (20–24). Accordingly, a therapeutic option that efficiently eradicates target cells expressing low levels of CD20 that survive rituximab or ofatumumab (ofa) therapy needs to be developed. Therefore, we developed a novel CD20-CAR and investigated the minimum threshold Ag expression level required for lysis of target cells and activation of CAR-T cells. To avoid possible immunological rejection against anti-mouse Abs, we used a humanized anti-CD20 mAb to construct CD20CAR (25). We also assessed its effects against tumor cell lines and primary cells isolated from mAb therapy-refractory, CD20-downregulated B cell tumors (24, 26, 27).

Materials and Methods

Cell lines

K562, CCRF-CEM, SU-DHL-4, SU-DHL-6, SU-DHL-10, Raji, RRBL1, and WILL2 cells were cultured in RPMI 1640 medium. OCI-Ly3 and OCI-Ly10 cells were kind gifts from Dr. K. Takeyama (Dana-Farber Cancer Institute, Boston, MA) and were cultured in IMDM (Sigma-Aldrich, St. Louis, MO). Each type of medium contained 10% FBS, 0.8 mM L-glutamine, and 1% penicillin-streptomycin. RRBL1 and WILL2 cells are cell lines established from a B cell lymphoma patient who exhibited CD20-negative phenotypic changes after repeated chemotherapy with rituximab (26, 27). CD20-transduced CCRF-CEM cell lines (CD20-CEMs) expressing various levels of CD20 were described elsewhere (28). CD20-transduced K562 (CD20-K562) cells were generated by retroviral transduction with the full-length CD20 molecule, as described (29).

Primary B cell tumor cells

Primary B cell tumor cells were obtained from PBMCs (CLL patient) or pleural effusion (lymphoma patient) according to protocols approved by the Institutional Review Board of Nagoya University School of Medicine, and written informed consent was obtained from each patient in accordance with the Declaration of Helsinki.

Quantification of CD20 molecules

CD20 molecules expressed on the surface of CD20-CEMs or other cell lines were quantified using quantitative immunofluorescence indirect assay (QIFIKIT; Dako, Glostrup, Denmark). Briefly, cells were stained with unlabeled anti-CD20 mouse mAb (BD Bioscience, San Jose, CA) or purified mouse IgG-κ (BioLegend, San Diego, CA) as an isotype control. The cells of interest and calibration beads from the kit were then simultaneously labeled with primary mAb, followed by FITC-conjugated goat anti-mouse secondary Ab staining. Labeled cells and calibration beads were analyzed on a flow cytometer, and a standard regression line between fluorescence intensity and Ag density that was expressed as Ab-binding capacity (ABC) in molecules per cell was calculated. Finally, the specific ABC (sABC) was determined by subtracting the background Ab equivalent of the isotype control from ABC (30).

Retroviral vector construction

CD20-binding scFv was constructed based on the reported sequences of the humanized anti-CD20 mAb (OUBM mAb) (25). OUBM mAb exhibits high CD20 binding affinity (K_D, 10.09 nM). H chain and L chain V region segments were linked with an 18-aa linker. scFv was then fused to a human IgG_4 hinge, a CD3-ζ chain, a CD28 costimulatory domain, and a truncated version of the epidermal growth factor receptor (tEGFR) that lacked epidermal growth factor binding and intracellular signaling domains downstream of the self-cleaving T2A sequence (31–33). By inserting the T2A sequence between CD20CAR and tEGFR, the two proteins were coexpressed at equimolar levels from a single transcript. Cell-surface tEGFR was detected using the biotinylated anti-EGFR mAb Erbitux (Bristol-Myers Squibb, New York, NY). The CD20CAR transgene was assembled by overlap extension PCR (34). CD20CAR was inserted into LZRS-pBMN-Z, using HindIII and NotI sites, and the CD20CAR-encoding retrovirus was produced using the Phoenix-Ampho system (Orbigen, San Diego, CA) and concentrated with Retro-X Concentrator (Clontech Laboratories, Mountain View, CA).

Generation, expansion, and selection of CD20CAR-transduced T cells

The PBMCs of a normal donor were isolated by centrifugation of whole blood using Ficoll-Paque (GE Healthcare, Wauwatosa, WI). $CD8^+$ lymphocytes were then purified with immunomagnetic beads (Miltenyi Biotec, Bergisch Gladbach, Germany), activated with anti-CD3/CD28 beads (Invitrogen, Carlsbad, CA), and transduced on day 3 after activation with the recombinant human fibronectin fragment (RetroNectin, Takara Bio, Otsu, Japan) by centrifugation at 2100 rpm for 45 min at 32°C with the retroviral supernatant (multiplicity of infection = 3). T cells were expanded in RPMI 1640 medium containing 10% human serum, 0.8 mM L-glutamine, 1% penicillin-streptomycin, and 0.5 μM 2-ME and supplemented with recombinant human IL-2 to a final concentration of 50 IU/ml. CAR-positive cells were enriched using immunomagnetic selection with biotin-conjugated anti-EGFR mAb and streptavidin beads (Miltenyi Biotec). The transduced T cells were expanded in culture by plating with γ-irradiated EBV-transformed lymphoblastoid cell line (LCL) at a T cell to LCL ratio of 1:7 and supplemented with IL-2 to 50 IU/ml (29).

Flow cytometry

All samples were analyzed with flow cytometry (FCM) on the FACSAria instrument (BD Biosciences), and data were analyzed using FlowJo software (Tree Star, Ashland, OR). Biotinylated Erbitux and streptavidin-PE were used to identify T cells that expressed tEGFR.

[^{51}Cr] release assay and coculture assay

For the [^{51}Cr] release assay, target cells were labeled for 2 h with [^{51}Cr] (PerkinElmer, Waltham, MA), washed twice, dispensed at 2×10^3 cells per well into triplicate cultures in 96-well round-bottom plates, and incubated for 4 h at 37°C with CD20CAR–T cells at various E:T ratios. Percent of specific lysis was calculated using a standard formula [(experimental − spontaneous release)/(maximum load − spontaneous release) × 100 (%)] and expressed as the mean of triplicate samples. Regarding the coculture assay, CEMs were labeled with 0.1 μM CFSE (Invitrogen), washed, and plated with CD20 CAR-T cells at a ratio of 1:1 without IL-2 supplementation. After a 72-h incubation, cells were stained with anti-CD8 mAb and analyzed with FCM. The percentages of CAR-T cells and CEMs within the live cell gates were assessed.

Intracellular cytokine staining and cytokine secretion assay

CD20CAR–T cells and K562 or CCRF-CEM cells that expressed CD20 were mixed at a 1:1 ratio in the presence of brefeldin A (Sigma-Aldrich) and then fixed and permeabilized with Cell Fixation/Permeabilization Kits (BD Biosciences) for intracellular cytokine assay. After fixation, T cells were stained with anti–IFN-γ and anti–CD8-allophycocyanin mAb (BD Biosciences). As a positive control for cytokine production, cells were stimulated with 10 ng/ml PMA and 1 μg/ml ionomycin (Sigma-Aldrich). CD20CAR–T cells and CEMs for the cytokine secretion assay were plated at an E:T ratio of 1:1, and IFN-γ, TNF-α, and IL-2 in the supernatant were measured with ELISA (BD Biosciences) after 16 h of incubation.

CFSE proliferation assay

CD20CAR–T cells were labeled with 0.2 μM CFSE, washed, and then plated with stimulator cells at a ratio of 1:1 without IL-2 supplementation. After a 72- or 96-h incubation, cells were stained with the anti-CD8 mAb, samples were analyzed with FCM, and the division of live $CD8^+$ T cells was assessed with CFSE dye dilution.

Intracellular phospho-flow analysis

CD20CAR–T cells and CD20-CEM cells expressing various levels of CD20 were mixed at a 1:5 ratio, centrifuged briefly, and incubated for various times at 37°C. Cells were then fixed by the addition of BD Cytofix Fixation Buffer at 37°C for 10 min, permeabilized in ice-cold BD Phosflow Perm Buffer III, and incubated on ice for 30 min (BD Biosciences). P-p44/42 MAPK (T202/Y204) or P-Zap-70 (Y319)/SyK(Y532) Rabbit Ab (Cell

Signaling Technology, Danvers, MA) and bovine anti-rabbit IgG-FITC as a secondary Ab (Santa Cruz Biotechnology, Dallas, TX) were used for phospho-specific staining.

Statistical analysis

Differences among results were evaluated with one-way or two-way ANOVA analysis and the Bonferroni test, as appropriate. Differences were considered significant when $p < 0.05$. Statistical analysis was performed using GraphPad Prism Version 5 software.

Results

Generation and functional analysis of CD20CAR-transduced T cells

To develop functional CD20CAR, we constructed CD20CAR consisting of anti–CD20-scFv linked to CD3ζ, a CD28 costimulatory domain, and a tEGFR; $CD8^+$ T cells were then retrovirally transduced with CD20CAR (Fig. 1A). After one course of stimulation and transduction, the expression of CD20CAR generally reached 40–80%. To determine transduction efficiency, CD20CAR and tEGFR were labeled with an anti-Fc Ab and biotinylated Erbitux, respectively. The expression of tEGFR reflected that of CAR on the transduced T cells, and we verified that the expression of CAR and tEGFR was similar after each transduction experiment (Fig. 1B) (32). Transduction efficiency could be monitored with tEGFR with high reproducibility (Fig. 1B, *right panel*). Using intracellular staining, we assessed the ability of CAR-T cells to produce IFN-γ in response to CD20. Stimulation with CD20-K562 cells induced robust production of IFN-γ, whereas mock-transduced K562 cells did not (Fig. 1C). These results demonstrated that CD20CAR–T cells recognized CD20 in an Ag-specific manner. After the transduction culture, CD20CAR-positive cells were enriched to a purity of >95% with biotinylated Erbitux and anti-biotin immunomagnetic beads (32), expanded by stimulating with a γ-irradiated LCL, and then used for subsequent experiments. The expression of CAR/tEGFR before and after LCL stimulation was sufficiently maintained (Fig. 1D). The ability of CD20CAR–T cells to lyse $CD20^+$ target cells was assessed after one course of transduction and expansion. CD20CAR–T cells specifically lysed CD20-K562 cells (Fig. 1E) in a highly reproducible manner (Fig. 1E, *right panel*). To examine background cytotoxicity, CD19CAR (non–target-specific CAR)–transduced T cells were examined for cytotoxicity against K562 or CD20-K562. Both experiments demonstrated almost the same range of cytotoxicity by the CD20CAR–T cells against K562 as in Fig. 1E. The range of cytotoxicity was 7–11% at an E:T ratio of 10:1 ($n = 4$). Two repeated LCL stimulations caused a log-scale expansion that resulted in 10,000-fold expansion of CD20CAR–T cells (Supplemental Fig. 1). The CD20CAR–T cells almost uniformly demonstrated effector phenotype ($CD28^-$, $CD62L^-$, $CD45RO^+$) after LCL stimulation (data not shown). In all subsequent experiments, $CD20CAR^-$ T cells were selected with tEGFR and expanded with one course of LCL stimulation; thus the transduction level of CD20CAR was uniformly >95% (Fig. 1D).

Quantification of CD20 molecules on the surface of CD20-CEMs and cell lines

Although CAR-T cells very efficiently recognize targets, the range of target molecule expression to which CAR-T cells can respond

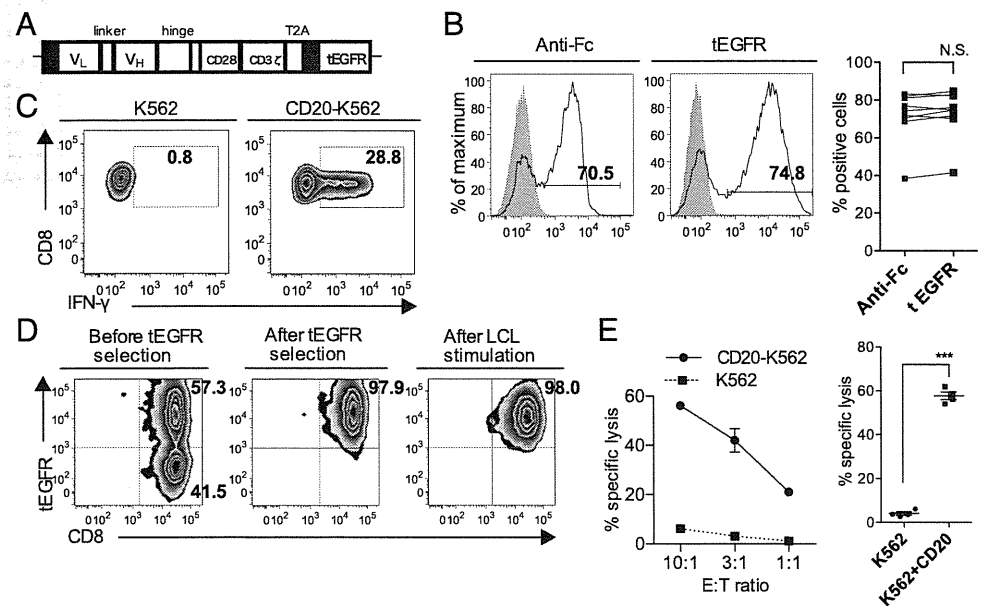

FIGURE 1. Construction, surface expression, and functional analysis of CD20CAR. (**A**) Schematic representation of the CD20CAR construct. CD20CAR consisted of anti-CD20 scFvs linked to CD3ζ, a CD28 costimulatory domain, and tEGFR as a transduction or selection marker via the T2A sequence. Solid black boxes denote the GM-CSF receptor leader sequence. Hinge, a human IgG4 hinge; linker, an 18-aa-long GGGS linker; V_H, H chain variable fragment; V_L, L chain variable fragment. (**B**) Surface expression of CD20CAR and tEGFR after transduction. $CD8^+$ cells were selected and transduced with the CD20CAR-encoding retrovirus supernatant. CD20CAR was stained with the anti-Fc Ab or biotinylated Erbitux, which reflects CAR expression. The surface expression of Fc/tEGFR was assessed on day 8 after one course of retroviral transduction. Gray-shaded histograms show staining of untransduced T cells. Representative flow plots are shown. *Right panel*, Data were pooled from nine independent experiments with T cells from eight donors (NS, paired *t* test). (**C**) Functional analysis of CD20CAR–T cells. On day 9 after transduction, CD20CAR–T cells were stimulated with either CD20-transduced K562 (CD20-K562) or mock-transduced K562 (K562) cells for 4 h at a 1:1 ratio, permeabilized, and then stained for IFN-γ. (**D**) Purity of CD20CAR–T cells before and after tEGFR selection and LCL stimulation. CD20CAR-positive cells were enriched by tEGFR selection and expanded by stimulation with γ-irradiated LCLs at a 1:7 ratio. Representative flow plots of three independent experiments from three donors are shown. (**E**) Cytotoxicity of CD20CAR–T cells. *Left panel*, After one course of expansion, cytotoxicity against either CD20-K562 or K562 cells was assessed at the indicated E:T ratio in the [^{51}Cr] release assay. The means ± SD of triplicate wells are shown. *Right panel*, Data were pooled from four independent experiments with CD20CAR–T cells from four donors (mean and SEM, ***$p < 0.0001$, the Student *t* test).

remains unknown (3–5). To assess this range more precisely, the number of CD20 molecules expressed on the cell surface of various cell lines was quantified as the CD20-specific Ab-binding capacity (CD20-sABC) on a per cell basis. We obtained 30 clones of CD20-CEMs expressing various levels of CD20 for use as target cells or stimulators (28). Of these, expression of CD20 by four representative clones was depicted, and the cells were used for several subsequent experiments as stimulators [CD20–very low CEM (VL-CEM) (CD20-mean fluorescence intensity [MFI]: 126/sABC: 240 molecules); CD20–low CEM (L-CEM) (CD20-MFI: 576/sABC: 5320 molecules); CD20–medium CEM (M-CEM) (CD20-MFI: 2396/sABC: 26,900 molecules); and CD20–high CEM (H-CEM) (CD20-MFI: 11,388/sABC: 142,722 molecules)] (Fig. 2A, Table I). The CD20-sABC values were 500,000 molecules for the germinal center B cell–type diffuse large B cell lymphoma (DLBCL)–derived cell lines; SU-DHL-4, -6, and -10, and 100,000 molecules for the non–germinal center B cell–type DLBCL-derived cell lines Ly-3 and -10 (Fig. 2B, Table I). RRBL1 and WILL2 are cell lines established from patients who experienced a relapse in B cell lymphoma with very weak expression of CD20 and who became resistant to rituximab (26, 27). The expression levels of CD20 by RRBL1 and WILL2 cells were 15,632

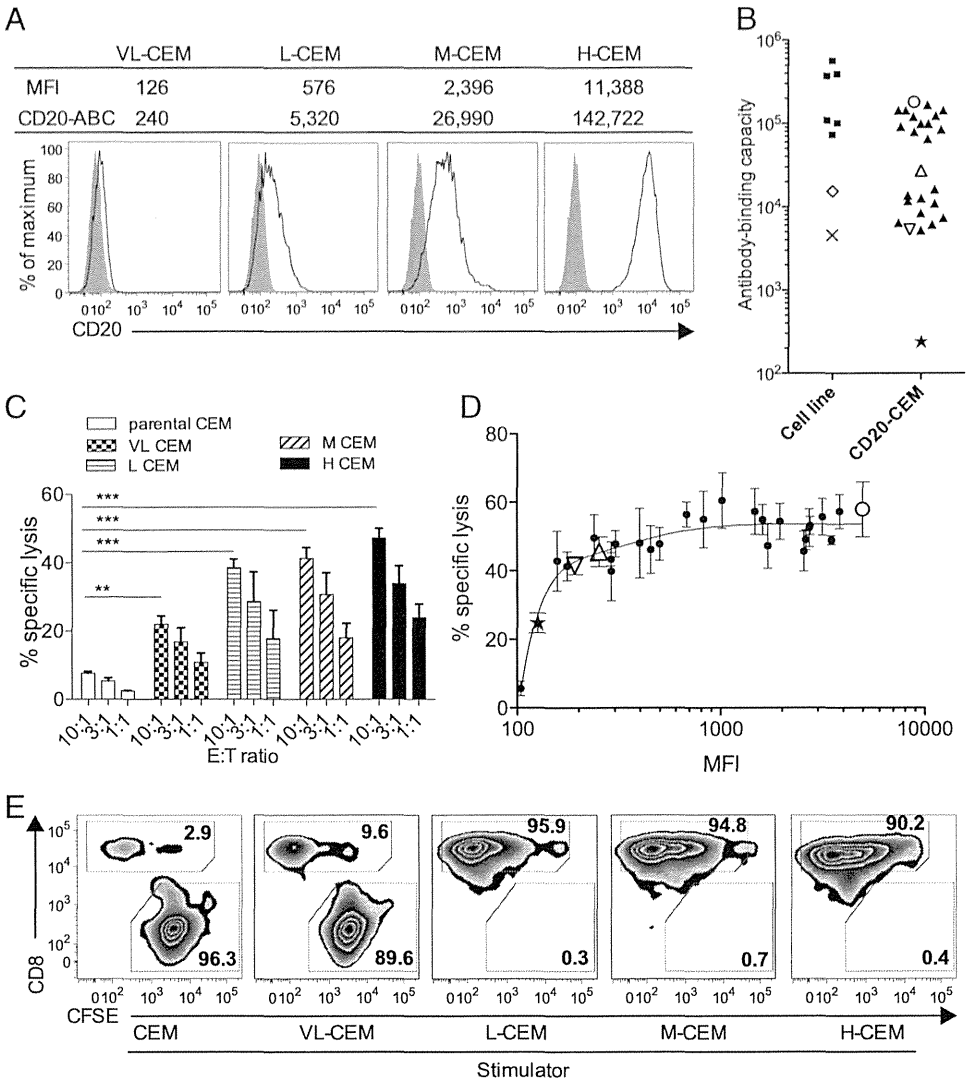

FIGURE 2. Quantification of CD20 molecules on the target cell surface and titration of the CD20 Ag expression level for CD20CAR–T cell cytotoxicity. (**A**) CD20 expression levels of the four representative CD20-CEM cell clones. The table above the histograms shows CD20-MFI and the quantification of CD20 molecules on each cell line as the Ab-binding capacity (CD20-ABC). Gray histograms show CD20 staining of untransduced CEM cells. VL-CEM, CD20-very low CEMs; L-CEM, CD20-low CEMs; M-CEM, CD20-medium CEMs; H-CEM, CD20-high CEMs. (**B**) Quantification of CD20 molecules on the surface of various cell lines. The number of CD20 molecules expressed on the surface of tumor cell lines was plotted in the left column (×, WILL2 cells; ◇, RRBL1 cells; ■, other cell lines). The number on CD20-CEMs is shown in the right column, including the four representative CEMs (★, VL-CEM; ▽, L-CEM; △, M-CEM; ○, H-CEM; ▲, other CD20-CEMs) (B, **D**). CD20-MFI data were analyzed in three independent experiments with similar results. CD20-MFI data in (A), (B), and (D) were collected in different experiments. (**C**) Cytotoxicity of CD20CAR–T cells against the four representative CD20-CEMs. Bars represent the cytotoxicity of CD20CAR–T cells against the four CD20-CEMs or untransduced CEMs (parental CEMs) at the indicated E:T ratios in the [^{51}Cr] release assay. The means ± SD of triplicate wells are shown (**$p < 0.01$, ***$p < 0.0001$, two-way ANOVA analysis). (D) The correlation between the CD20-MFI of CD20-CEMs and the cytotoxicity of CD20CAR–T cells. The cytotoxicity of CD20CAR-T cells against each CD20-CEM cell line was determined as in (C). The cytotoxicity of each CD20-CEM cell line at an E:T ratio of 10:1 was plotted against the CD20-MFI of CD20-CEMs. Data were pooled from four independent experiments with CD20CAR–T cells from four donors (mean and SEM). The solid line represents the fitted curve obtained with the nonlinear regression model using Prism5 software. (**E**) CD20CAR–T cells eradicated CD20-CEMs in coculture assays according to CD20 expression levels. CAR-T cells and CFSE-labeled CEMs were cultured in a 1:1 ratio without IL-2 supplementation for 72 h. The percentage of surviving CAR–T cells and residual CEMs within the live cell gates are shown. Data are representative of three independent experiments using three independent CD20CAR–T cell lines.

Table I. Surface CD20 expression of CD20-CEMs and other tumor cell lines

	MFI	sABC
CEM		
Parental	121	0
#2	9,683	120,208
#3	11,403	142,921
#4	6,905	83,978
#7	7,491	91,567
#19	14,228	180,597
#23	1,293	13,675
#27	11,388	142,722
#29	8,045	98,770
#31	15,550	198,366
#37	845	8,414
#47	1,209	12,680
#71	563	5172
#72	6,494	78,675
#73	8,049	98,822
#76	126	240
#82	641	6,062
#85	9,922	123,353
#94	576	5,320
w6	15,672	200,009
w7	13,180	166,571
w12	1,063	10,960
w40	5,414	64,824
w54	17,930	230,546
w114	1,125	11,689
w127	749	7,303
w132	1,497	16,104
w141	669	6,383
w147	2,396	26,990
w149	11,363	142,390
Tumor cell line		
RRBL1	1,436	15,376
WILL2	510	4,571
DHL-4	33,076	390,664
DHL-6	31,713	371,994
DHL-10	6,983	564,656
Ly-3	6,798	73,049
Ly-10	9,206	100,965
Raji	9,949	108,985

and 4869 molecules per cell, respectively (Fig. 2B, ◇ and ×, respectively). Relative to other cell lines, CD20-CEMs represented a very wide range of CD20 expression, from 240 to 230,546 molecules per cell, which was considered very low to high (Fig. 2B, Table I).

To evaluate the potential influence of costimulation, inhibitory signals, and adhesion molecule, the expression of CD80, CD86, CD54 (ICAM-1), CD58 (leukocyte function–associated molecule-3), and PD-L1 on target tumor cells was investigated. CEM cells demonstrated a tolerogenic phenotype, expressing low levels of CD80 and CD86 and relatively high levels of the inhibitory ligand PD-L1. CD54 was positive in all examined cell lines, whereas CD58 was negative in WILL2 cells (Supplemental Fig. 2) (35).

Determination of the minimum threshold of CD20 expression that CAR-T cells require for recognition and lysis

The level of CD20 Ag expression for rituximab-induced complement-dependent cytotoxicity (CDC) was determined using the same set of CD20-CEMs (28). We performed the rituximab-induced CDC assay and obtained almost the same results using human complement (Supplemental Fig. 3A). As demonstrated previously, Ab-dependent cellular cytotoxicity (ADCC) with rituximab against CD20-CEMs did not show a clear threshold of CD20 expression (data not shown) (28). CD20-CEMs with an MFI <1000 (equivalent to sABC of 10^4) did not induce significant CDC, whereas CD20-CEMs with an MFI of 1000–3000 (equivalent to sABC of 10^4–10^5) did. CD20-CEMs with an MFI >3000 effectively induced cytotoxicity, and maximal CDC was obtained at an MFI >5000 (sABC of 10^5) (Supplemental Fig. 3A). CDC induced by the humanized anti-CD20 mAb OUBM was also examined. OUBM mAb, with which CD20CAR was constructed, induced marked CDC with half-maximum cytotoxicity at a CD20 expression level similar (MFI of 3000) to that of rituximab (MFI of 3000) (Supplemental Fig. 3).

In contrast to the weak CDC caused by rituximab and OUBM mAb, CD20-CEMs were more efficiently lysed by CD20CAR–T cells, with the exception of VL-CEMs, which underwent a significantly lower degree of lysis (Fig. 2C).

To determine the threshold expression level of the CD20 Ag required to induce CAR-T cytotoxicity, we performed a [^{51}Cr] release assay with CD20CAR–T cells against the clones of CD20-CEMs expressing various levels of CD20 (CD20-MFI: 126–6924/CD20-sABC: 240–230,546 molecules). CD20CAR–T cells lysed VL-CEMs, which had the lowest level of CD20 (MFI: 126/sABC: 240 molecules, 22.8 ± 2% lysis). In addition, CD20CAR–T cells induced similar lysis (40–60% lysis) of various CD20-CEMs with higher expression of CD20 (CD20-MFI: 157/CD20-sABC: ≥5172 molecules, E:T ratio of 10:1) (Fig. 2D). CD20CAR–T cells exhibited efficient cytotoxicity against CD20-CEMs with an MFI <1000; at this level, rituximab and OUBM mAb did not induce significant CDC (Supplemental Fig. 3A, 3B, Fig. 2D). Half-maximum cytotoxicity by CD20CAR–T cells was observed at an MFI of ~200–300 (equivalent to sABC of 10^3). Therefore, the minimum threshold number of surface target molecules that CAR-T recognized and lysed was markedly low, at approximately a few hundred molecules.

A coculture assay was performed as a more physiological model. In this assay, CD20CAR–T cells partially, but not completely, eradicated VL-CEMs. Conversely, CAR-T cells completely eradicated L-, M-, and H-CEMs after a 72-h coculture (Fig. 2E).

Intracellular signaling, cytokine production, and cell division after stimulation with the four representative CD20-CEMs

An advantage of CAR-T cell therapy over mAb therapy is that CAR-T cells can become activated and proliferate upon specific stimulation of the target Ag, enabling CAR-T cells to exhibit long-lasting efficacy in vivo (1, 3–5, 9). Although we titrated the threshold Ag density for CAR-T–induced lysis, the threshold for cytotoxicity and full activation, including cytokine production and proliferation, are uncoupled in Ag-specific T cells (36). Thus, we examined the threshold Ag density for CAR-T activation. To define the minimum threshold of CD20 expression that was needed for effective activation and expansion of CAR-T cells, we examined phosphorylation of the signaling molecules ERK and ZAP70 after stimulation with the four representative CD20-CEMs. The CD20-CEMs, except for VL-CEMs, induced similar phosphorylation of ERK (pERK) and ZAP70 in CAR-T cells (Fig. 3A and data not shown). pERK was equally upregulated when CAR-T cells were stimulated with L-, M-, and H-CEMs, but not with VL-CEMs, after 10 min (Fig. 3A). Time-course analysis showed that the pERK MFI responses were almost equal after L-, M-, and H-CEM stimulation, and the peak time was 5–10 min after stimulation. Nevertheless, VL-CEM induced only minimal phosphorylation of ERK in CAR-T cells, similar to that of parental CEMs (Fig. 3A, 3B).

Cytokine production and proliferation were evaluated following different stimuli. Stimulation with VL-CEM did not induce the production of cytokines from CAR-T cells. Conversely, L-, M-, and H-CEMs induced equivalent production of IFN-γ (Fig. 3C–E), IL-2 (Fig. 3F, 3G), and TNF-α (Fig. 3H). IL-2 production after H-CEM

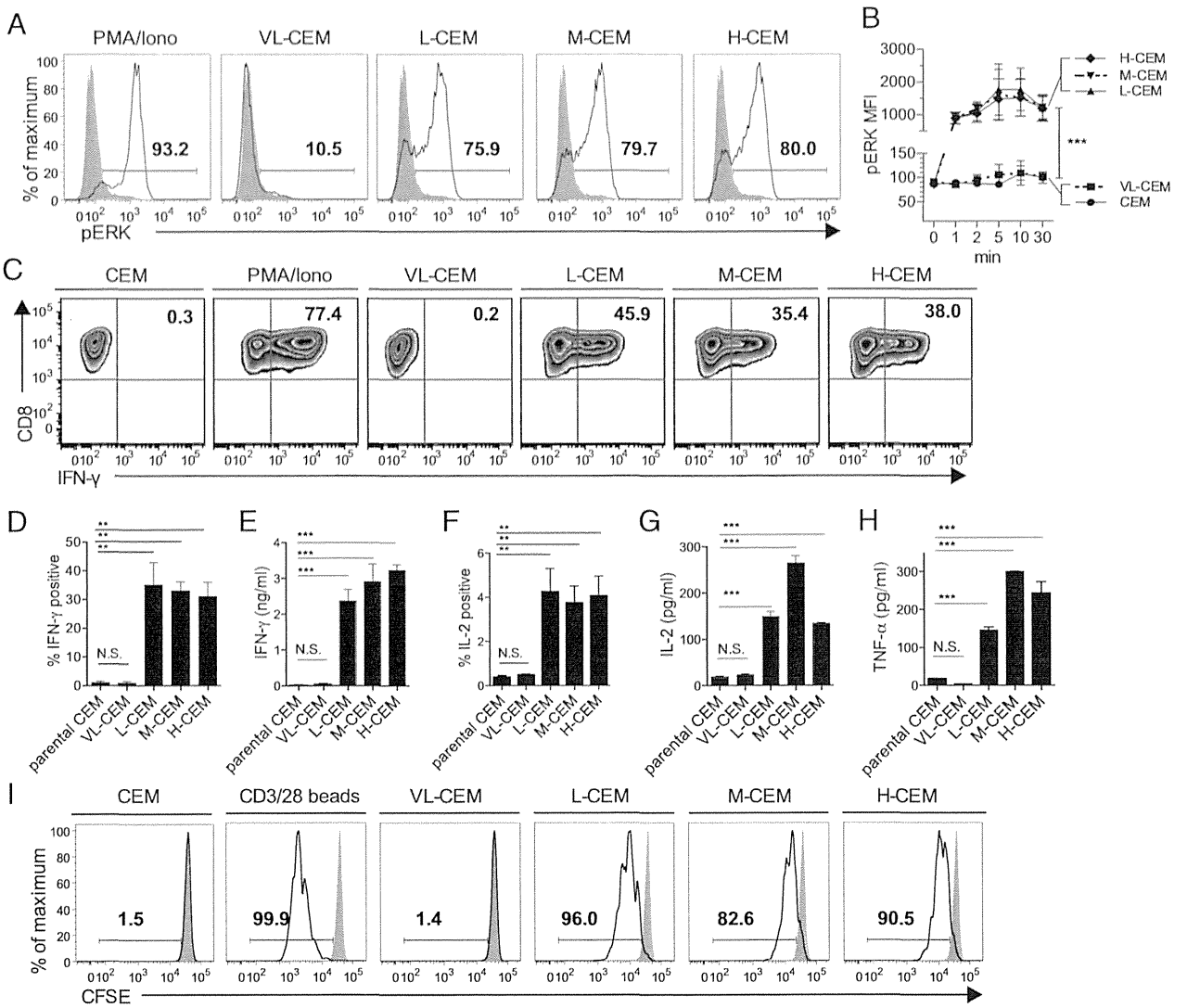

FIGURE 3. Titration of the threshold of CD20 expression for CD20CAR–T cell activation upon stimulation. (**A**) Phosphorylation of a distal signaling molecule, ERK (pERK). CD20CAR–T cells were stimulated with the four representative CD20-CEMs, untransduced CEMs at a responder to stimulator ratio of 1:5, or PMA/ionomycin (Iono) for 10 min, and were then fixed, permeabilized, and stained with pERK-specific Ab. Gray histograms show data obtained from T cells stimulated with parental CEMs. (**B**) Time-course analysis of pERK. The phosphorylation of ERK in CD20CAR–T cells was analyzed 1, 2, 5, 10, and 30 min after stimulation with the four representative CD20-CEMs or parental CEMs at a 1:5 ratio. MFI of pERK after stimulation is shown. Data were pooled from three independent experiments with CD20CAR–T cells from three donors. Means and SEM are shown (***$p < 0.0001$, two-way ANOVA analysis). (**C**) IFN-γ production after stimulation. CD20CAR–T cells were stimulated with the four representative CD20-CEMs, parental CEMs at a 1:1 ratio, or PMA/Iono for 4 h, and were then permeabilized and stained for IFN-γ. (**D** and **F**) The percentages of T cells that stained positive for IFN-γ and IL-2, respectively, are shown. Data were pooled from three independent experiments with CD20CAR–T cells from three donors (mean and SEM, **$p < 0.01$). The secretion of (**E**) IFN-γ, (**G**) IL-2, and (**H**) TNF-α upon CD20-CEM stimulation. CD20CAR–T cells were stimulated with the indicated CEMs at a 1:1 ratio, and culture supernatants were harvested at 16 h and analyzed with ELISA (mean and SEM, ***$p < 0.001$, one-way ANOVA). (**I**) Division of CD20CAR–T cells upon CD20 ligation. CD20CAR–T cells were labeled with CFSE and stimulated with CD20-CEMs, untransduced CEMs, or anti-CD3/28 beads at a 1:1 ratio, and the CFSE staining intensity was then analyzed with FCM 96 h after stimulation. Gray histograms show data of nonstimulated CD20CAR–T cells. Data are representative of at least three independent experiments with CD20CAR–T cells from three donors (A, C, and I).

stimulation was approximately half that after M-CEM stimulation in repeated experiments ($n = 3$). Because we observed no significant difference in intracellular IL-2 production (Fig. 3F), the low IL-2 concentration after H-CEM stimulation may have reflected an increase in cytokine consumption. Regarding proliferation, VL-CEM did not induce cell division of CAR-T cells, whereas other CEMs induced efficient cell division 72 and 96 h after stimulation (Fig. 3I and data not shown). The kinetics of CD20CAR–T cell division increased with higher CD20 expression on CD20-CEMs, but the percentages of proliferating cells were equivalent among L-, M-, and H-CEM stimulation (Fig. 3I). The kinetics of division appeared to be partly dependent on target Ag density (Fig. 3I).

Taken together, the minimum threshold required to induce activation and proliferation of CAR-T cells was between the levels expressed by VL-CEMs and L-CEMs. This threshold was very low: less than the CD20 expression level of L-CEMs (CD20-MFI: 576/CD20-sABC: 5320). CD20 expression above the threshold significantly activated CAR-T cells.

Effects on CD20^{lo} cell lines and CD20^{lo} primary tumor cells isolated from patients with rituximab-refractory B cell lymphoma

Because we demonstrated that CD20CAR–T cells recognized markedly low expression of CD20, we examined the effectiveness of

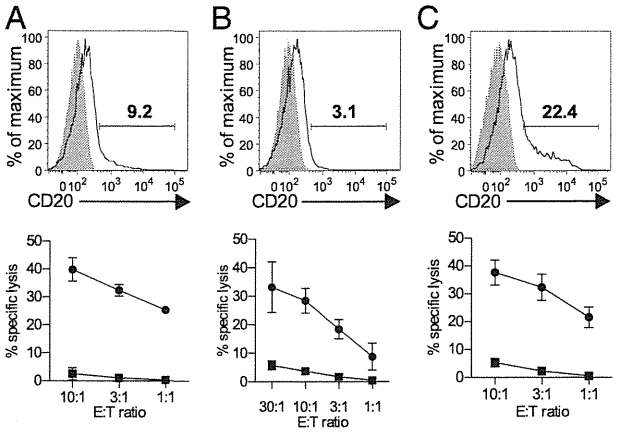

FIGURE 4. Cytotoxicity of CD20CAR–T cells against CD20-downregulated tumor cell lines and primary lymphoma cells. (**A** and **B**) CD20 expression and cytotoxicity by CD20CAR–T cells against CD20-downregulated tumor cell lines RRBL1 and WILL2, respectively. (**C**) CD20 expression and cytotoxicity by CD20CAR–T cells against primary tumor cells isolated from the pleural effusion of a patient with rituximab-refractory B cell lymphoma. Throughout the figure, *upper panels* show CD20 staining (solid line), isotype control staining (gray shaded), and percentages of CD20-positive fractions. *Lower panels* show the cytotoxicity by CD20CAR–T cells against the cell lines at the indicated E:T ratios in the [^{51}Cr] release assay. The means ± SEM of three independent experiments with CD20CAR–T cells from three donors are shown. • and ■ denote cytotoxicity by CD20CAR-T and untransduced T cells, respectively.

CD20CAR–T cell therapy against CD20^{lo} tumor cells. First, the cytotoxicity of CD20CAR–T cells against CD20^{lo} tumor cell lines was investigated. CD20CAR–T cells lysed both CD20^{lo} cell lines, RRBL1 and WILL2, very efficiently (Fig. 2B, 4A, 4B, *lower panel*).

We also evaluated cytotoxicity against CD20^{lo} primary cells from a patient with DLBCL (double-hit lymphoma). The patient exhibited disease recurrence after a full course of R-hyper CVAD (37), and lymphoma cells were obtained from pleural effusion. At the time of relapse, CD20 expression was reduced in most cells, and only ~20% of cells showed low CD20 expression (Fig. 4C, *upper panel*). CD20CAR–T cells efficiently lysed CD20^{lo} primary DLBCL cells. This lytic activity was higher than the percentage of the CD20^{+} cell fraction, suggesting that CD20CAR–T cells partially lysed the cell fraction expressing low levels of CD20 (Fig. 4C, *lower panel*).

CD20CAR–T cells recognized and lysed residual CLL cells after ofa therapy

CLL is a chronic lymphoproliferative disease in which the anti-CD20 mAb is a choice for standard care (38). The expression of CD20 by CLL cells is generally lower than that of other CD20^{+} lymphoid malignancies such as ALL and lymphoma (39). To compare the potency of CD20 recognition by anti-CD20 mAb, we examined cytotoxicity and cytokine production following stimulation of CD20-downregulated CLL cells. Before starting mAb therapy, the expression of CD20 by CLL cells was intact, and the lytic activity of CD20CAR–T cells was remarkable (Fig. 5A). The patient then became chemorefractory following repeated administration of rituximab (the clinical course of this patient is summarized in Supplemental Fig. 4). In this patient, CLL cells could not be controlled with rituximab-combined chemotherapy. The expression of CD20 by CLL cells decreased, and the MFI showed two peaks: the nearly negative fraction and the CD20 low fraction (Fig. 5B, *upper panel*). However, cytotoxicity by CD20CAR–T cells was maintained (Fig. 5B, *lower panel*). The patient was then treated with the novel anti-CD20 mAb ofa (40). A marked decrease in the number of CLL cells and regression of lymphadenopathy were observed after a single course of ofa, whereas the CD20 very low fraction, which was confirmed to consist of CD5^{+} CLL cells (data not shown), remained in the peripheral

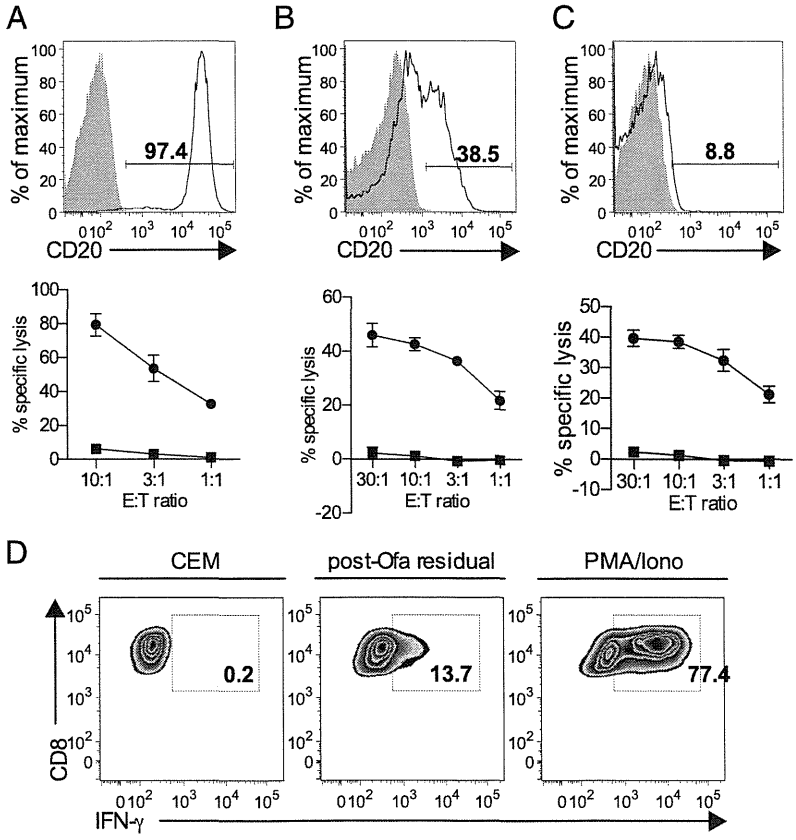

FIGURE 5. Cytotoxicity of CD20CAR–T cells against CD20-downregulated primary CLL cells. (**A–C**) CD20 expression and cytotoxicity against CLL cells isolated from an untreated patient (A), before administration of ofa (preofa) (B), and 14 d after the 10th course of ofa (postofa) (C). CLL cells were isolated from the peripheral blood of a patient with rituximab-refractory CLL. Residual CLL cells after rituximab treatment were isolated from the peripheral blood of a patient at two different time points, pre- and postofa. *Upper panels* show CD20 staining (solid line) and isotype control staining (gray shaded). *Lower panels* show cytotoxicity by CD20CAR–T cells against CLL cells at the indicated E:T ratios in the [^{51}Cr] release assay. Filled circles and squares denote cytotoxicity by CD20CAR-T and untransduced T cells, respectively. The means ± SEM of three independent experiments with CD20CAR–T cells from three donors are shown (A–C). (**D**) Cytokine production by CD20CAR–T cells upon stimulation with postofa CLL cells. CD20CAR–T cells were stimulated with postofa CLL cells, parental CEMs at a 1:1 ratio, or PMA/Iono for 4 h, and were then permeabilized and stained for IFN-γ.

blood. We obtained residual CLL cells from the peripheral blood of the patient after the 10th course of ofa. After ofa treatment, the CD20 relatively low fraction disappeared, and CD20 expression by CLL cells was almost uniformly nearly negative (Fig. 5C, *upper panel*). The residual cells were exposed once to the mAb therapy and survived. Therefore, the CD20 expression level of the residual cells was considered to be below the effective range of rituximab or ofa. In the [^{51}Cr] release assay using these primary CLL cells, CD20CAR–T cells efficiently recognized and lysed not only CLL cells before ofa but also CLL cells after ofa (Fig. 5B, 5C, *lower panel*). With an intracellular IFN-γ assay, after ofa, stimulation of CD20CAR–T cells with CLL cells, which were nearly CD20-negative, induced production of IFN-γ by CD20CAR–T cells (Fig. 5D).

Discussion

In the current study, we generated a novel CD20CAR based on a humanized anti-CD20 mAb (25). CD20CAR–T cells specifically and effectively lysed CD20-positive target cells. The expression of CD20CAR was precisely evaluated using the anti-Fc Ab and biotinylated Erbitux. Although we did not directly evaluate the copy number of the CD20CAR transgene, the variation observed in lytic activity against K562-CD20 cells was very low following tEGFR selection, suggesting that the expression of CD20CAR was similar among the CD20CAR–T cell lines. With cytotoxicity analysis of CD20CAR–T cells against CD20-CEMs expressing various levels of CD20, we first titrated the minimum threshold of CD20 expression that CAR-T cells could recognize and lyse. We demonstrated that CD20CAR–T cells lysed CD20-CEMs with CD20-ABC = 240 molecules, which was the lowest CD20 level in this set. This level was 1000-fold lower than that required to induce CDC with rituximab and OUBM mAb. The difference in cytolytic activity between CDC and CAR should mostly depend on the presence or absence of effector cells. Although CDC and CAR activity is similar against CD20-high CEM cells, CD20CAR–T cells demonstrated far better lytic activity than CDC against CD20-low CEM cells (Fig. 2D, Supplemental Fig. 3). This finding suggested that CAR-T therapy might show better effect in the case of only a limited number of target Ags on the tumor cells. The correlation between CD20-ABC and specific lysis was also represented with a saturation curve, which had a sharp inclination against CD20^{lo} targets. This phenomenon was attributed to CAR technology providing full activation with CD3ζ and the simultaneous costimulation of CD28 (3–6).

We next determined the threshold of CD20 expression that could activate and expand CD20CAR–T cells upon stimulation with the representative CD20-CEMs. Although cytotoxicity analysis revealed that CD20CAR–T cells lysed VL-CEMs, these cells did not induce downstream signaling, production of IFN-γ, or proliferation of CAR–T cells. Stimulation with L-, M-, and H-CEMs (CD20-ABC: ≥5320 molecules) effectively and equally activated CD20CAR–T cells. Taken together, these results indicated that the threshold of CD20 expression for recognition and lysis by CD20CAR–T cells, which we termed the "lytic threshold," was a few hundred molecules, and the threshold required for activation and expansion of CAR-T cells, termed the "activating threshold," was slightly higher, at a few thousand molecules. These results are consistent with previous findings in which the lytic threshold and activating threshold were different in TCR activation (36). Because endogenous T cells such as melanoma-specific T cells and virus-specific T cells require 10–100 epitope molecules per target cell to trigger specific lysis (13), both the lytic threshold and the activating threshold were slightly lower in endogenous T cells compared with CAR-T cells. Obviously, the thresholds are affected by the affinity of the mAb or TCR for the ligand or peptide/HLA complex. In our study, the affinity of the humanized anti-CD20 mAb (OUBM mAb), which was used to construct CD20CAR, was within the same range as that of rituximab (K_D value: OUBM mAb, 10.09 nM; rituximab, 5.35 nM) (25). Using a mAb with this range of affinity, both thresholds of CAR-T cells were close to those of endogenous T cells. Furthermore, CD20CAR–T cells recognized and lysed CD20-downregulated target cells that survived after mAb therapy, indicating that manufacturing a CAR with a mAb may reinforce target recognition more than the mAb itself.

The epitope location of the mAb is another important issue. Ofa exposure before sample collection may account for the apparent CD20 downregulation. However, we confirmed CD20 downregulation using another CD20 mAb, a B9E9 clone in which the epitope location is distinct from that of ofa (23). This confirmation indicated that CD20 downregulation after ofa treatment was not caused by competition between the analytical Ab and ofa. The epitope location targeted by OUBM mAb and ofa partially overlaps, but that of OUBM mAb and rituximab does not (25). Therefore, ofa can theoretically block the ligation of CD20CAR-T but rituximab cannot. We observed that CD20CAR–T cells indeed lysed CD20-downregulated target cells both after rituximab and ofa, suggesting that the potential effect of epitope blocking was minor in the current study.

The results of the current study led us to propose a novel concept for future searches for target Ag in CAR-T therapy. Suitable target Ags for CAR-T cell therapy are considerably different from those for mAb therapy in terms of their expression profiles and levels. Higher expression levels on the surface of tumor cells have been considered in target Ag searches for mAb therapy because off-tumor expression is usually negligible (41). However, for the target of CAR-T cell therapy, off-tumor expression of the target molecules must be strictly negative or at a very low level that is below the lytic threshold, at a few hundred molecules. Otherwise, severe adverse effects could occur as a result of off-tumor effects (10). The target Ag safety in the context of mAb therapy does not necessarily translate into the safety of Ag in the context of markedly more sensitive CAR-T cell therapy (10). Conversely, even if the threshold was below the mAb therapy range, low Ag expression above the activating threshold, such as at a few thousand molecules, could be considered a candidate for the target Ag of CAR-T cell therapy.

Acquired resistance to rituximab has become a problem in the treatment of patients with CD20-positive B cell tumors (20, 23). One suggested mechanism is downregulation of CD20 (20, 22, 26). A total of 15–20% of relapsed patients exhibit CD20 Ag loss, as observed with immunohistochemistry analysis in samples taken at relapse (20, 23). Our CD20CAR–T cells recognized and lysed primary cells isolated from patients with mAb therapy–refractory lymphoma and CLL, although the expression level of CD20 was very low. We also analyzed CD20CAR-T recognition against CD20-downregulated, mAb-refractory CLL in detail (21). The residual cells after CD20 mAb therapy expressed significantly low levels of CD20, and this expression level must have been below the effective range of the mAb in principle. CD20CAR–T cells lysed both postrituximab and postofa residual CLL cells, indicating that CD20CAR–T cells have a greater potential to recognize the target than mAbs. Even residual postofa CLL cells stimulated CD20CAR–T cells, and thus we conclude that the very low expression of CD20 on CLL cells could still efficiently provide stimulation for the further repopulation of CD20CAR–T cells.

In other CAR therapies targeting CD19, several patients were reported to have relapsed despite the completely negative con-

version of the Ag molecule after CAR-T cell therapy (2). Although CAR-T cells recognize very low levels of the target Ag, they cannot recognize completely Ag-negative cells. The strategy of administering CAR-T therapy as a first-line treatment, or in earlier phases with the aim of earlier eradication of target cells, may prevent immunological escape by negative conversion of the Ag.

One limitation of the current study is that we assessed the threshold using only CD20 and CD20CAR systems. Because the threshold may be influenced by many other factors, such as affinity (42), structure (43), epitope localization of individual CAR-Ag pairs (44, 45), and the expression of a coreceptor on target cells (46), the threshold may vary among mAbs and target Ags. We also could not investigate the relationship between the expression of CD20 and the ADCC activity of mAbs because NK cell activity is predominant in the CD20-CEM system, and a clear threshold has not been observed (28). Although the potential relationship between target Ag density and ADCC activity has been investigated in other experimental systems, $>10^4$ Ag molecules per cell are needed to demonstrate significant ADCC (47). In the current study, the minimum threshold of CAR recognition was 3-log units lower than that of mAbs to trigger CDC. CAR can also directly mobilize T cells to target cells, whereas mAb therapy mainly depends on indirect cytotoxicity such as CDC or ADCC (3–5, 19, 28). Thus, the lytic and activating thresholds of CAR are considered significantly lower than those of mAbs.

We concluded that CAR-T cells can recognize and lyse cells expressing considerably low levels of the target Ag and were activated and expanded upon such stimulation. CD20CAR–T cell therapy may also be applicable for the treatment of CD20-positive lymphoid malignancies.

Acknowledgments

We thank Yoko Matsuyama, Asako Watanabe, and Chika Wakamatsu for technical assistance.

Disclosures

H.K. has received research funding from Bristol-Myers Squibb, Chugai Pharmaceutical, Kyowa Hakko Kirin, Dainippon Sumitomo Pharma, Zenyaku Kogyo, and FUJIFILM. The other authors have no financial conflicts of interest.

References

1. Porter, D. L., B. L. Levine, M. Kalos, A. Bagg, and C. H. June. 2011. Chimeric antigen receptor-modified T cells in chronic lymphoid leukemia. *N. Engl. J. Med.* 365: 725–733.
2. Grupp, S. A., M. Kalos, D. Barrett, R. Aplenc, D. L. Porter, S. R. Rheingold, D. T. Teachey, A. Chew, B. Hauck, J. F. Wright, et al. 2013. Chimeric antigen receptor-modified T cells for acute lymphoid leukemia. *N. Engl. J. Med.* 368: 1509–1518.
3. Sadelain, M., R. Brentjens, and I. Riviere. 2013. The basic principles of chimeric antigen receptor design. *Cancer Discov.* 3: 388–398.
4. Jensen, M. C., and S. R. Riddell. 2014. Design and implementation of adoptive therapy with chimeric antigen receptor-modified T cells. *Immunol. Rev.* 257: 127–144.
5. Turtle, C. J., M. Hudecek, M. C. Jensen, and S. R. Riddell. 2012. Engineered T cells for anti-cancer therapy. *Curr. Opin. Immunol.* 24: 633–639.
6. Kowolik, C. M., M. S. Topp, S. Gonzalez, T. Pfeiffer, S. Olivares, N. Gonzalez, D. D. Smith, S. J. Forman, M. C. Jensen, and L. J. Cooper. 2006. CD28 costimulation provided through a CD19-specific chimeric antigen receptor enhances in vivo persistence and antitumor efficacy of adoptively transferred T cells. *Cancer Res.* 66: 10995–11004.
7. Imai, C., K. Mihara, M. Andreansky, I. C. Nicholson, C. H. Pui, T. L. Geiger, and D. Campana. 2004. Chimeric receptors with 4-1BB signaling capacity provoke potent cytotoxicity against acute lymphoblastic leukemia. *Leukemia* 18: 676–684.
8. Zhong, X. S., M. Matsushita, J. Plotkin, I. Riviere, and M. Sadelain. 2010. Chimeric antigen receptors combining 4-1BB and CD28 signaling domains augment PI3kinase/AKT/Bcl-XL activation and $CD8^+$ T cell-mediated tumor eradication. *Mol. Ther.* 18: 413–420.
9. Kochenderfer, J. N., M. E. Dudley, S. A. Feldman, W. H. Wilson, D. E. Spaner, I. Maric, M. Stetler-Stevenson, G. Q. Phan, M. S. Hughes, R. M. Sherry, et al. 2012. B-cell depletion and remissions of malignancy along with cytokine-associated toxicity in a clinical trial of anti-CD19 chimeric-antigen-receptor-transduced T cells. *Blood* 119: 2709–2720.
10. Morgan, R. A., J. C. Yang, M. Kitano, M. E. Dudley, C. M. Laurencot, and S. A. Rosenberg. 2010. Case report of a serious adverse event following the administration of T cells transduced with a chimeric antigen receptor recognizing ERBB2. *Mol. Ther.* 18: 843–851.
11. Hudis, C. A. 2007. Trastuzumab—mechanism of action and use in clinical practice. *N. Engl. J. Med.* 357: 39–51.
12. Ménard, S., P. Casalini, M. Campiglio, S. M. Pupa, and E. Tagliabue. 2004. Role of HER2/neu in tumor progression and therapy. *Cell. Mol. Life Sci.* 61: 2965–2978.
13. Purbhoo, M. A., D. H. Sutton, J. E. Brewer, R. E. Mullings, M. E. Hill, T. M. Mahon, J. Karbach, E. Jäger, B. J. Cameron, N. Lissin, et al. 2006. Quantifying and imaging NY-ESO-1/LAGE-1-derived epitopes on tumor cells using high affinity T cell receptors. *J. Immunol.* 176: 7308–7316.
14. Liddy, N., G. Bossi, K. J. Adams, A. Lissina, T. M. Mahon, N. J. Hassan, J. Gavarret, F. C. Bianchi, N. J. Pumphrey, K. Ladell, et al. 2012. Monoclonal TCR-redirected tumor cell killing. *Nat. Med.* 18: 980–987.
15. Sadelain, M., R. Brentjens, and I. Rivière. 2009. The promise and potential pitfalls of chimeric antigen receptors. *Curr. Opin. Immunol.* 21: 215–223.
16. Thomas, D. A., S. O'Brien, S. Faderl, G. Garcia-Manero, A. Ferrajoli, W. Wierda, F. Ravandi, S. Verstovsek, J. L. Jorgensen, C. Bueso-Ramos, et al. 2010. Chemoimmunotherapy with a modified hyper-CVAD and rituximab regimen improves outcome in de novo Philadelphia chromosome-negative precursor B-lineage acute lymphoblastic leukemia. *J. Clin. Oncol.* 28: 3880–3889.
17. Jaglowski, S. M., L. Alinari, R. Lapalombella, N. Muthusamy, and J. C. Byrd. 2010. The clinical application of monoclonal antibodies in chronic lymphocytic leukemia. *Blood* 116: 3705–3714.
18. Abramson, J. S., and M. A. Shipp. 2005. Advances in the biology and therapy of diffuse large B-cell lymphoma: moving toward a molecularly targeted approach. *Blood* 106: 1164–1174.
19. Jazirehi, A. R., and B. Bonavida. 2005. Cellular and molecular signal transduction pathways modulated by rituximab (rituxan, anti-CD20 mAb) in non-Hodgkin's lymphoma: implications in chemosensitization and therapeutic intervention. *Oncogene* 24: 2121–2143.
20. Hiraga, J., A. Tomita, T. Sugimoto, K. Shimada, M. Ito, S. Nakamura, H. Kiyoi, T. Kinoshita, and T. Naoe. 2009. Down-regulation of CD20 expression in B-cell lymphoma cells after treatment with rituximab-containing combination chemotherapies: its prevalence and clinical significance. *Blood* 113: 4885–4893.
21. Jilani, I., S. O'Brien, T. Manshuri, D. A. Thomas, V. A. Thomazy, M. Imam, S. Naeem, S. Verstovsek, H. Kantarjian, F. Giles, et al. 2003. Transient down-modulation of CD20 by rituximab in patients with chronic lymphocytic leukemia. *Blood* 102: 3514–3520.
22. Tsai, P. C., F. J. Hernandez-Ilizaliturri, N. Bangia, S. H. Olejniczak, and M. S. Czuczman. 2012. Regulation of CD20 in rituximab-resistant cell lines and B-cell non-Hodgkin lymphoma. *Clin. Cancer Res.* 18: 1039–1050.
23. Johnson, N. A., S. Leach, B. Woolcock, R. J. deLeeuw, A. Bashashati, L. H. Sehn, J. M. Connors, M. Chhanabhai, A. Brooks-Wilson, and R. D. Gascoyne. 2009. CD20 mutations involving the rituximab epitope are rare in diffuse large B-cell lymphomas and are not a significant cause of R-CHOP failure. *Haematologica* 94: 423–427.
24. Shimada, K., A. Tomita, S. Saito, and H. Kiyoi. 2014. Efficacy of ofatumumab against rituximab-resistant B-CLL/SLL cells with low CD20 protein expression. *Br. J. Haematol.* 166: 455–457.
25. Uchiyama, S., Y. Suzuki, K. Otake, M. Yokoyama, M. Ohta, S. Aikawa, M. Komatsu, T. Sawada, Y. Kagami, Y. Morishima, and K. Fukui. 2010. Development of novel humanized anti-CD20 antibodies based on affinity constant and epitope. *Cancer Sci.* 101: 201–209.
26. Tomita, A., J. Hiraga, H. Kiyoi, M. Ninomiya, T. Sugimoto, M. Ito, T. Kinoshita, and T. Naoe. 2007. Epigenetic regulation of CD20 protein expression in a novel B-cell lymphoma cell line, RRBL1, established from a patient treated repeatedly with rituximab-containing chemotherapy. *Int. J. Hematol.* 86: 49–57.
27. Sonoki, T., Y. Li, S. Miyanishi, H. Nakamine, N. Hanaoka, H. Matsuoka, I. Mori, and H. Nakakuma. 2009. Establishment of a novel CD20 negative mature B-cell line, WILL2, from a CD20 positive diffuse large B-cell lymphoma patient treated with rituximab. *Int. J. Hematol.* 89: 400–402.
28. van Meerten, T., R. S. van Rijn, S. Hol, A. Hagenbeek, and S. B. Ebeling. 2006. Complement-induced cell death by rituximab depends on CD20 expression level and acts complementary to antibody-dependent cellular cytotoxicity. *Clin. Cancer Res.* 12: 4027–4035.
29. Terakura, S., T. N. Yamamoto, R. A. Gardner, C. J. Turtle, M. C. Jensen, and S. R. Riddell. 2012. Generation of CD19-chimeric antigen receptor modified $CD8^+$ T cells derived from virus-specific central memory T cells. *Blood* 119: 72–82.
30. Lenkei, R., J. W. Gratama, G. Rothe, G. Schmitz, J. L. D'hautcourt, A. Arekrans, F. Mandy, and G. Marti. 1998. Performance of calibration standards for antigen quantitation with flow cytometry. *Cytometry* 33: 188–196.
31. Kumar, A., E. T. Petri, B. Halmos, and T. J. Boggon. 2008. Structure and clinical relevance of the epidermal growth factor receptor in human cancer. *J. Clin. Oncol.* 26: 1742–1751.
32. Wang, X., W. C. Chang, C. W. Wong, D. Colcher, M. Sherman, J. R. Ostberg, S. J. Forman, S. R. Riddell, and M. C. Jensen. 2011. A transgene-encoded cell surface polypeptide for selection, in vivo tracking, and ablation of engineered cells. *Blood* 118: 1255–1263.
33. Szymczak-Workman, A. L., K. M. Vignali, and D. A. Vignali. 2012. Design and construction of 2A peptide-linked multicistronic vectors. Cold Spring Harb. Protoc. 2012(2): 199–204.

34. Andris-Widhopf, J., P. Steinberger, R. Fuller, C. Rader, and C. F. Barbas, 3rd. 2011. Generation of human scFv antibody libraries: PCR amplification and assembly of light- and heavy-chain coding sequences. *Cold Spring Harb. Protoc.* 2011(9).
35. Weijtens, M. E., R. A. Willemsen, B. A. van Krimpen, and R. L. Bolhuis. 1998. Chimeric scFv/gamma receptor-mediated T-cell lysis of tumor cells is coregulated by adhesion and accessory molecules. *Int. J. Cancer* 77: 181–187.
36. Faroudi, M., C. Utzny, M. Salio, V. Cerundolo, M. Guiraud, S. Müller, and S. Valitutti. 2003. Lytic versus stimulatory synapse in cytotoxic T lymphocyte/target cell interaction: manifestation of a dual activation threshold. *Proc. Natl. Acad. Sci. USA* 100: 14145–14150.
37. Oki, Y., J. R. Westin, F. Vega, H. Chuang, N. Fowler, S. Neelapu, F. B. Hagemeister, P. McLaughlin, L. W. Kwak, J. E. Romaguera, et al. 2013. Prospective phase II study of rituximab with alternating cycles of hyper-CVAD and high-dose methotrexate with cytarabine for young patients with high-risk diffuse large B-cell lymphoma. *Br. J. Haematol.* 163: 611–620.
38. Hallek, M., B. D. Cheson, D. Catovsky, F. Caligaris-Cappio, G. Dighiero, H. Döhner, P. Hillmen, M. J. Keating, E. Montserrat, K. R. Rai, and T. J. Kipps. International Workshop on Chronic Lymphocytic Leukemia. 2008. Guidelines for the diagnosis and treatment of chronic lymphocytic leukemia: a report from the International Workshop on Chronic Lymphocytic Leukemia updating the National Cancer Institute-Working Group 1996 guidelines. *Blood* 111: 5446–5456.
39. Prevodnik, V. K., J. Lavrenčak, M. Horvat, and B. J. Novakovič. 2011. The predictive significance of CD20 expression in B-cell lymphomas. *Diagn. Pathol.* 6: 33.
40. Wierda, W. G., S. Padmanabhan, G. W. Chan, I. V. Gupta, S. Lisby, and A. Osterborg, Hx-CD20-406 Study Investigators. 2011. Ofatumumab is active in patients with fludarabine-refractory CLL irrespective of prior rituximab: results from the phase 2 international study. *Blood* 118: 5126–5129.
41. Scott, A. M., J. D. Wolchok, and L. J. Old. 2012. Antibody therapy of cancer. *Nat. Rev. Cancer* 12: 278–287.
42. Turatti, F., M. Figini, E. Balladore, P. Alberti, P. Casalini, J. D. Marks, S. Canevari, and D. Mezzanzanica. 2007. Redirected activity of human antitumor chimeric immune receptors is governed by antigen and receptor expression levels and affinity of interaction. *J. Immunother.* 30: 684–693.
43. Hudecek, M., M. T. Lupo-Stanghellini, P. L. Kosasih, D. Sommermeyer, M. C. Jensen, C. Rader, and S. R. Riddell. 2013. Receptor affinity and extracellular domain modifications affect tumor recognition by ROR1-specific chimeric antigen receptor T cells. *Clin. Cancer Res.* 19: 3153–3164.
44. Haso, W., D. W. Lee, N. N. Shah, M. Stetler-Stevenson, C. M. Yuan, I. H. Pastan, D. S. Dimitrov, R. A. Morgan, D. J. FitzGerald, D. M. Barrett, et al. 2013. Anti-CD22-chimeric antigen receptors targeting B-cell precursor acute lymphoblastic leukemia. *Blood* 121: 1165–1174.
45. Long, A. H., W. M. Haso, and R. J. Orentas. 2013. Lessons learned from a highly-active CD22-specific chimeric antigen receptor. *OncoImmunology* 2: e23621.
46. Casucci, M., B. Nicolis di Robilant, L. Falcone, B. Camisa, M. Norelli, P. Genovese, B. Gentner, F. Gullotta, M. Ponzoni, M. Bernardi, et al. 2013. CD44v6-targeted T cells mediate potent antitumor effects against acute myeloid leukemia and multiple myeloma. *Blood* 122: 3461–3472.
47. Tang, Y., J. Lou, R. K. Alpaugh, M. K. Robinson, J. D. Marks, and L. M. Weiner. 2007. Regulation of antibody-dependent cellular cytotoxicity by IgG intrinsic and apparent affinity for target antigen. *J. Immunol.* 179: 2815–2823.